Seasonal Hydrologic and Biogeochemical Drivers of Nutrient Availability in Urban Green Spaces

Isabelle R. Horvath
Marquette University

SEASONAL HYDROLOGIC AND BIOGEOCHEMICAL DRIVERS OF NUTRIENT AVAILABILITY IN URBAN GREEN SPACES

By

Isabelle Horvath

A Thesis submitted to the Faculty of the Graduate School,

Marquette University,

In Partial Fulfillment of the Requirements for

The Degree of Master of Science

Milwaukee, Wisconsin

December 2020

ABSTRACT

SEASONAL HYDROLOGIC AND BIOGEOCHEMICAL DRIVERS OF NUTRIENT AVAILABILITY IN URBAN GREEN SPACES

Isabelle R. Horvath

Marquette University, 2020

Humans dominate urban nutrient cycles – adding nitrogen (N) and phosphorus (P) through car exhaust, fertilizer over-use, and pet waste. N and P are transported to streams via stormwater runoff, where they create eutrophic conditions and reduced water quality. Urban green spaces, like green stormwater infrastructure (GSI), have potential to mitigate N and P pollution through retention in soils and plants. Nutrient retention is accomplished in urban green spaces through filtration, plant uptake, and biogeochemical processes. These processes are highly variable, due to the influence of varying environmental drivers, such as temperature, rainfall, soil moisture, and soil redox status. This work studies seasonal variation in nutrient mobility and corresponding hydrologic and biogeochemical conditions in urban soils. Ion exchange resins were used to capture the seasonality of soil nutrient availability. Environmental drivers such as soil and air temperature, soil moisture, soil oxygen, and precipitation were also monitored. Sites included a green roof, upland and lowland plots in a constructed wetland, and an urban garden in Milwaukee. Using multiple linear regression models, different environmental drivers predicted nutrient availability across sites. High nitrate pulses occurred in the wetland lowland in the summer following dry conditions, which contrasted low and stable nitrate availability in the wetland upland. Across all upland sites, phosphate mobilization was strongly correlated with precipitation, indicating mobilization of soil phosphorus pools. These patterns indicate varying roles of hydrologic and biogeochemical drivers for N and P availability in urban green spaces. The observed relationships can be used to better understand nutrient retention and dynamics in urban green spaces under variable hydrological and biogeochemical conditions.

AWKNOWLEDGMENTS

Isabelle R. Horvath

My sincere gratitude goes out to the many people who personally and professionally assisted me in the completion of this Thesis. My thanks first extend to my advisor, Dr. Anthony Parolari, and my thesis committee. Dr. Parolari, thank you for your commitment to my academic career, betterment as a researcher, and for your leadership and encouragement on this project. Drs. Mayer and McDonald thank you for your time spent on this thesis, and especially for your perceptive feedback and questions.

My gratitude is also extended to the many students whose direct work and support made this project successful. Thank you, undergraduate students Gerardo Ornelas-Rodriguez, Kamila Turczewski, and Garrett Leverentz, for applying your time, passion, curiosity, and arm strength to the project and carrying of batteries. Thank you also to alumni Laine Pulvermacher and graduate student Thuy (Duyen) Lam for your hard work installing and maintaining sensors, as well as for your endless support through my thesis experience. I have also been blessed with the support, constructive critique, and words of affirmation and validation from the many people whom I have had the pleasure of working with over the course of my Masters: thank you especially Daniella Castillo, Joe Naughton, Sazzad Sharior, Spencer Sebo, Elizabeth Regier, Nate Hay, Caitlin Lulay, Colin Wilson, and Kun Zhang.

This work would not have been possible without the support from Fund for Lake Michigan, thank you for your investment in research and in the future of stormwater management through supporting this project. Thank you also to the staff at the Marquette University Discovery Learning Center, especially Tom Silman for your patience and assistance. Additional thanks to the Marquette University Water Quality Center for assistance acclimating to the space, and especially to Mike Dollhopf, Donald Ryan, and Kaushik Venkiteshwaran for their technical expertise and consultation.

Finally, thank you to my family and friends, who never ceased to encourage me to follow wherever my passions lead, no matter how many states away they may lie. Thank you for your support, for the many times you listened to my research challenges and practice presentations, reassured me of my capability, and explained to the people in your lives what “stormwater” is, I’m forever grateful.

TABLE OF CONTENTS

LIST OF TABLES

LIST OF FIGURES

1. INTRODUCTION

1.1 Problem Statement

Diffuse nutrient management is a wicked problem (Lintern, McPhillips, Winfrey, Duncan, & Grady, 2020; Patterson, Smith, & Bellamy, 2013). The release of the nutrients nitrogen (N) and phosphorous (P) from non-point, or diffuse, anthropogenic urban and agricultural sources into the environment is the major cause of eutrophication in surface waters (Howarth, Sharpley, & Walker, 2002; Stets et al., 2020). In the Great Lakes region alone, eutrophication has had public health and recreational impact as seen through compromised drinking water quality in Toledo, Ohio (Wines, 2014) and the creation of dead zones in Green Bay, Wisconsin (Bergquist, 2018).

When nutrients accumulate in receiving water bodies in excess, they lead to compromised environmental health, and decline in economic and recreational value of waters through the promotion of eutrophication and harmful algal bloom growth (Anderson, Glibert, Patricia, & Burkholder, 2002; Carpenter, 2008; Heisler et al., 2008). Nutrients overstimulate aquatic ecosystem productivity, leading to oxygen depletion that threatens aquatic wildlife (Bennett, Carpenter, & Caraco, 2001; Ho & Michalak, 2017; Khan & Ansari, 2005). Eutrophication impacts not only critical aquatic ecology, but also human health, as algal toxins can impact drinking water safety (Heisler et al., 2008) and the economy via reduced property values and recreation opportunities (Dodds et al., 2009; Dodds & Smith, 2016).

Even with knowledge of the high consequences of eutrophication, the management of diffuse nutrient pollution remains a challenge because of legislative and engineering

barriers. The Clean Water Act prohibits the discharge of any pollutant from any "point source" into navigable waters except under permit, but there is no address of non-point source pollution in the Act (33 U.S.C. §1251). Stormwater that pollutes surface waters from non-point-source entry is not directly regulated. From an engineering perspective, non-point sources are difficult to treat because the sources of the pollution are landscape-based, and thus widely dispersed. Thus, regulatory means have succeeded in diminishing nutrient loading to water bodies from point sources, but non-point sources remain an incessant challenge as they are unregulated, leaving non-point sources as the focal point for further mitigation of eutrophication (Ator, Webber, & Chanat, 2020; Dodds & Smith, 2016; McGrath, Comerford, & Duryea, 2000; Michalak et al., 2013; Pataki et al., 2011; Schindler, Carpenter, Chapra, Hecky, & Orihel, 2016; Stets et al., 2020).

The issue of nutrient pollution is perpetuated by the context of an increasingly urban society and related resource scarcity (Allenby, 2012). Increasing urbanization results in ever increasing impervious area, which alters both hydrology of stormwater conveyance, and also impacts nutrient cycling as infiltration is prevented and increased anthropogenic pollutants are added to stormwater (Lintern et al., 2020). Humans add nutrients to the urban landscape through N additions like N-based fertilizers, fossil fuel use in vehicles, and P additions like pet and yard waste (Hobbie et al., 2017). Transport of these nutrients via stormwater displaces landscape nutrients, resulting in both straining nutrient resources on land and hyper loading water bodies to a harmful extent (Amundson et al., 2015). Thus the management of diffuse nutrients falls under the US National Academy of Engineering grand challenge of restoring balance to the N cycle ("NAE Grand Challenges," n.d.), as well as aligning with UN Sustainability Goals 6: "Clean

Water and Sanitation", 11: "Sustainable Cities and Communities" and 14: "Life Below Water" (Lintern et al., 2020; "Sustainable Development Goals," 2020).

To prevent eutrophication and rise to the challenges presented by urbanization and altered nutrient cycles it is necessary to improve the understanding of nutrient cycling in urban landscapes. Urban areas are distinct from rural in their landcover, engineered drainage, high impact of human activity, and influence of social values on urban ecology (Kaye, Groffman, Grimm, Baker, & Pouyat, 2006; Pataki et al., 2011). In the urban environment, impervious surfaces like roads, roofs, and other infrastructure, while not themselves contributing nutrients, propagate the issue of nutrient pollution by increasing runoff production, and preventing the infiltration of nutrients. Therefore, impervious land cover, or green spaces, are responsible for processing nutrients in urban areas, or acting as "sinks" for nutrients in the larger picture of an urban nutrient system flooded with human-driven nutrient "sources." With an imbalance of urban nutrient sinks and sources, it is critical to understand the mechanisms that drive nutrient cycling in urban green spaces in order to best use these nutrients sinks to prevent loading of nutrients in water bodies (Groffman et al., 2017; Lintern et al., 2020; Pataki et al., 2011).

Nutrient processing in the urban landscape is driven by various biogeochemical and hydrological mechanisms, and these mechanisms are subject to seasonality. As with natural systems, urban green spaces have varying nutrient processing capacities due to seasonality (Buffam, Mitchell, & Durtsche, 2016; Mullins et al., 2020). Changes in season in natural (non-urban) areas dictate how nutrients are processed through the influence of seasonal changes on (or "seasonality of") groundwater table movement, soil microbial activity, plant activity, soil moisture fluctuations and weathering (Duncan,

Band, Groffman, & Bernhardt, 2015; Trentman, Tank, Jones, Mcmillan, & Royer, 2020). Advances in the management of diffuse urban nutrient pollution require a better understanding of how nutrients are processed (Lintern et al., 2020). To have a more complete understanding of the function and variability of nutrient processing of urban green spaces, it is necessary to understand the seasonality of nutrient processing in these spaces.

1.2 Thesis Objective

The goal of this research was to identify the role of various environmental controls on the availability of nutrients in urban green spaces. Observing the seasonality of nutrient availability will give insight as to when nutrients may be leaching from urban soils. Identifying significant relationships between environmental drivers and nutrient mobility can help to distinguish specific biogeochemical mechanisms responsible for observed seasonality, and thus provide a foundation for urban green space design improvements for enhanced nutrient retention.

2. LITERATURE REVIEW

2.1 Introduction

Urban areas, from the combined effects of high anthropogenic nutrient release and low landscape permeability, contribute to eutrophication. Humans increase nutrient loading through atmospheric deposition, fertilizer use, food waste, yard waste, pet waste and fossil fuel burning (Hobbie et al., 2017; Kaye et al., 2006). Human manipulations of the landscape also alter nutrient cycling in urban areas, particularly the development of impervious areas, connected impervious areas and compaction of pervious surfaces, which impede landscape nutrient processing (Boardman, Efi, Dolph, & Finlay, 2019; Carey et al., 2013), and through urban landscaping like urban trees (Janke, Finlay, & Hobbie, 2017) and green stormwater infrastructure (GSI) (LeFevre et al., 2015). Human-built pervious landscapes may act as sources or sinks of nutrients (Carey et al., 2013; Hurley, Shrestha, & Cording, 2017; L. McPhillips et al., 2018; Nidizgorski & Hobbie, 2016; Pouyat, Forest, Yesilonis, & Forest, 2007).

Understanding urban nutrient processing requires the study of sources and sinks of nutrients in the urban landscape (Carey et al., 2013). Urban green spaces include features like vacant lots, lawns, gardens, parks and GSI (Nidizgorski & Hobbie, 2016; Pataki et al., 2011; Sevostianova & Leinauer, 2014; Wang, Haver, & Pataki, 2014). While all these urban green spaces are potential contributors in the processing of urban diffuse nutrients, this review focuses on GSI, as these practices are “hot spots” for nutrient processing in urban landscapes, and have been the primary focus of research on urban diffuse nutrient management. This literature review will identify the state of

knowledge in urban nutrient processing through GSI. This is accomplished by highlighting foundations of GSI, variability in GSI performance, and seasonality of GSI removal and retention performance.

The second part of this review provides historical background and scientific context for the use of ion exchange resins (IERs) for this project. IER use is novel in the field of urban ecohydrology and this review provides background and justification for their use in this field, and details the knowledge gained by using these monitoring tools, and their limitations.

2.2 GSI Foundational Knowledge

2.2.1 GSI Definition and Terminology

Green stormwater infrastructure (GSI) is defined by the Clean Water Act as "…the range of measures that use plant or soil systems, permeable pavement or other permeable surfaces of substrates, stormwater harvest and reuse, or landscaping to store, infiltrate, or evapotranspiration stormwater and reduce flows to sewer systems or to surface water" (The Clean Water Act, 1977). GSI is also labeled or encompassed in terms like Best Management Practices (BMPs) (Lintern et al., 2020), Green Infrastructure (GI), Urban Ecological Infrastructure (UEI), Blue-Green Infrastructure (BGI) (Childers et al., 2019), Stormwater Control Measures (SCM) (Erickson, Taguchi, & Gulliver, 2018), Stormwater Management Practices (SMPs) (LeFevre et al., 2015) and Low Impact Development (LID) (Lucas & Sample, 2015). In addition to their water quantity treatment capacity, many GSI practices also serve to improve water quality (LeFevre et al., 2015; Tzoulas et al., 2007).

GSI practices range greatly in size, design, goal, and names, and have varying performance expectation depending on types. GSI practices attributed with water quality treatment capacity include ponds, wetlands, bioretention, and infiltration practices (Center for Watershed Protection, 2007). It is widely acknowledged that all GSI pollutant removal efficiencies are affected by inflow concentration, age of the practice, and concurrent volume reduction in addition to variation based on GSI system type (Center for Watershed Protection, 2007; Department of Environmental Conservation, 2015). Many resources have been established to summarize GSI performance based on practice type, including the International Stormwater Best Management Practices Database and state-specific stormwater design manuals.

2.2.2 GSI Nutrient Removal Performance

Nutrient removal performance ranges among GSI practices and nutrients, but it is generally accepted that removal of dissolved nutrients is more variable than suspended or particulate nutrients (LeFevre et al., 2015). Dissolved nutrient removal is variable because of the sensitivity of biogeochemical factors responsible for water quality treatment to site-specific characteristics like soil moisture, soil organic matter, carbon access, soil oxygen, and vegetation type, to name a few (Griffiths & Mitsch, 2017; Lucas & Greenway, 2008, 2011; L. McPhillips et al., 2018; Pataki et al., 2011). In general, removal of suspended pollutants (L. McPhillips et al., 2018; Morse, McPhillips, Shapleigh, & Walter, 2017; Pataki et al., 2011) and heavy metals (Gill, Ring, Higgins, & Johnston, 2014; Hunt et al., 2012; Walker & Hurl, 2002) is better than dissolved nutrient removal (Dietz & Clausen, 2005, 2006; Hsieh, Davis, & Needelman, 2007; Kim, Seagren, & Davis, 2003; LeFevre et al., 2015; Lintern et al., 2020; Yan, Davis, Asce, &

James, 2016). N and P are the nutrients of primary interest in GSI research because of their potential for stimulating eutrophication.

Retention and removal of the dissolved N species ammonium and nitrate have often been attributed to denitrification, in which nitrate is transformed to N-gas via anaerobic microbial activity. Dissolved N species in stormwater include nitrate, nitrite, ammonium, ammonia, and organic N (LeFevre et al., 2015). In the context of bioretention media, denitrification can occur depending on the soil redox status of the soil, a factor driven by soil oxygen content in the soil, which is influenced by soil moisture (Davis, Shokouhian, Sharma, & Minami, 2006; Kim et al., 2003). The promotion of denitrification in GSI practice for nitrate removal has been explored in both modeled (Norton, Harrison, Keller, & Moffett, 2017) and field (L. McPhillips & Walter, 2015) observations. It has been found that storm frequency (Norton et al., 2017), status of the soil moisture as predominantly dry or saturated (Bledsoe, Bean, Austin, & Peralta, 2020; L. McPhillips & Walter, 2015), and seasonal groundwater fluctuations (Mullins et al., 2020) control denitrification rates in GSI. Further, it has been cautioned that the promotion of saturated, anaerobic denitrification zones in GSI can contribute to greenhouse gas (GHG) emissions as incomplete denitrification can result in the emission of the potent GHG nitrous oxide and methane (Bledsoe et al., 2020; L. E. McPhillips, Groffman, Schneider, & Walter, 2016; L. McPhillips et al., 2018). A further concern is the necessary consideration of particulate N when accounting for dissolved N leaching from GSI, as particulate organic nitrogen can also be transformed to dissolved organic nitrogen, and the uptake of this N species is not addressed with denitrification efforts, but

it can be a significant source of N loss in GSI systems (LeFevre et al., 2015; L. Li & Davis, 2014).

Dissolved P leaching has been observed from many studies of GSI, leading to recent research in amendments for enhanced P adsorption. Dissolved P includes inorganic orthophosphates and organic phosphorous, where orthophosphate is biologically available (LeFevre et al., 2015). Phosphorous export is largely due to the presence of P in the soil media. Leaf litter from system foliage, use of mulch as a top layer, and compost in the soil media can load GSI with P and result in P leaching (Hunt et al., 2012; Hurley et al., 2017; LeFevre et al., 2015; J. Li & Davis, 2016). There are two dominant P retention mechanisms in GSI: 1) fast reversible sorption or 2) predominantly one-direction, irreversible sorption of P onto metal oxides (LeFevre et al., 2015). To promote lasting sorption of P in GSI recent research has sought to apply metal oxide sorption through the addition of materials high in metal oxides in GSI soil as an "amendment" for enhanced P retention. Iron filings (Erickson, Gulliver, & Weiss, 2007, 2012), water treatment residue, fly ash (LeFevre et al., 2015), and industrial solid wastes (You et al., 2019) are examples of amendment materials that have been used in infiltration and bioretention systems to promote the sorption of P onto metal oxides. These soil amendments have shown improved P retention, reaching removal rates from 50-97% (Erickson et al., 2012; You et al., 2019). P leaching can also be mitigated through GSI system maintenance in which organic matter is removed from the system before it decomposes, thus removing excess P loading from non-stormwater sources (Drapper & Hornbuckle, 2018; Erickson et al., 2018).

2.3 Seasonality of Nutrient Processing

2.3.1 Nutrient Seasonality in Natural Systems

Nutrient dynamics are known to be seasonal. Multiple studies have classified seasonal nutrient concentration profiles in stream water quality based off seasonally driven landscape processing of nutrients. It has been shown that forested areas of the southern US have summer nitrate peaks, whereas northern area nitrate stream concentrations peak in the winter (Band, Tague, Groffman, & Belt, 2001; Brookshire, Gerber, Webster, Vose, & Swank, 2011; Mulholland, 1997; Murdoch & Stoddard, 1992). A watershed in Maryland that yielded summertime seasonal highs was investigated for root causes of nitrate peaks, where it was determined that summertime evapotranspiration and water table decline created well-aerated, nitrifying soil conditions, leading to high nitrate production in proximal riparian soils (Duncan et al., 2015). Seasonal impact of nutrient processing on water quality has also been linked to land use type in the Great Lakes, where natural and agricultural watersheds export nutrients to surface water in phase with discharge (spring peaks and summer lows), whereas urban land use types display aseasonal nutrient phasing (Van Meter, Chowdhury, Byrnes, & Basu, 2019).

2.3.2 Nutrient Seasonality in GSI

Ecosystem functions are dependent on the seasonality of mechanisms that drive ecosystem function, and thus it is expected that GSI practices also display seasonal variability. The most common effect of seasonality on nutrient removal is the influence of warm summertime temperatures on microbial metabolism and plant uptake, resulting in higher summertime uptake of dissolved, bioavailable nutrients (Roseen, Robert et al., 2009; Walaszek, Bois, Laurent, Lenormand, & Wanko, 2018). However, the reverse had

also been observed, where summertime nutrients are higher than during other seasons. These summertime peaks have been attributed to the induction of nitrification from seasonally driven low-oxygen conditions in a roadside trench (Mullins et al., 2020), and microbial mineralization and seasonally promoted weathering at a green roof (Buffam et al., 2016). Seasonally varying nutrient removal has also been attributed to seasonally varying precipitation volumes and associated stormwater quality concentrations (Griffiths & Mitsch, 2017; Walaszek et al., 2018). In general, colder-weather GSI performance is worse than in warm-weather conditions (Roseen, Robert et al., 2009; Sohn, Kim, Li, & Brown, 2019).

2.4 Monitoring Techniques

Monitoring the in-situ availability of nutrient ions is possible with ion exchange resins (IERs). Ion exchange resins are synthetic charged polymers that can sorb available ions to their surface through ion exchange.

IERs were first used for measuring nutrient availability in the 1950s, and have since been applied to measure plant available nutrients in soils, and the rates at which they are released (Qian & Schoenau, 2002). Qian & Schoenau (2002) found over 400 peer-reviewed journal articles applying IERs for nutrient availability measurements. The use of IERs offer the advantage of consideration of kinetics and transport, accurate representation of availability, and ease-of-use (Qian & Schoenau, 2002). IER use began with resin beads and became available in membrane form, called ion exchange membranes (IEMs), in the 1960s (Meason & Idol, 2008). IERs are now widely available in both bead and membrane form.

IERs measure the availability of ions in soils, where uptake is reflective of 3 factors: lability of the ions (status as free or unbound), mobility of the ions (ability to traverse through soil pores), and comparative ion strength of the IER and soil demands (Figure 1). IERs function by exchanging weakly bound ions with ions with a higher affinity onto the charged resin surface. Weakly bonded ions are loaded onto the IER surface to be stripped off by ions with higher ionic strength in soils ("PRS Technology," 2020). In order for this exchange to occur, the ions in soil must not be taken up by or bonded to other charged matter, like being used by plants or microbes, or bound to metals or soil particles (Cooperband & Logan, 1994; Krause & Ramlal, 1987; Qian & Schoenau, 2002). Further, soil ions must come into contact with the resins, a process which can occur through advective transport in pore water or by diffusion (Cooperband, Gale, & Comerford, 1999; Qian & Schoenau, 2002). The final factor contributing to IER measurement of nutrients is the competition between ionic strength of the resin, and in-situ demands for ions after they have sorbed to the IER. While initially conceived as "infinite sinks" of available nutrients, IERs cease to sorb ions by reaching a saturation point if buried too long, or if greater demand for the ions is present in the soil (Meason & Idol, 2008; Qian & Schoenau, 2002, 2007). Due to this potential limitation in ion sorption and potential for desorption, "infinite sinks" is a misleading conceptual description for IERs. IERs can instead be conceived as "dynamic exchangers" because ions both sorb and desorb from IERs, to reach an equilibrium with soil demands (McGrath et al., 2000; Qian & Schoenau, 2002). Thus IERs measure available ions, those ions which are both labile and mobile, and reflect the cumulative availability of these ions over the time

period where IERs were buried, considering equilibration with soil demands that overcome the ionic strength of the IER (Figure 1).

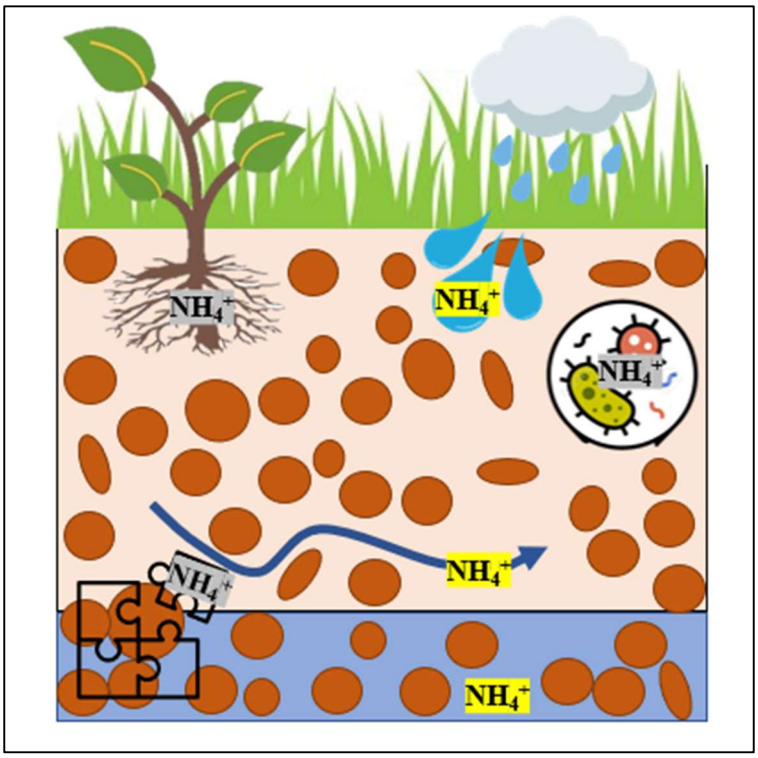

Figure 1: Available nutrients in a soil system. Nutrients in a soil system must be both labile and mobile to be detected by IERs. Nutrients both available and labile, and therefore mobile, are highlighted in yellow. Available nutrients are free in the soil system and able to move through either precipitation, pore water movement or through groundwater. Unavailable nutrients, highlighted in grey, as they are bound or used by mechanisms like plant uptake, microbial metabolism, or physical adsorption on soil particles.

IER bags and IEMs adhere to the same functional principles, but due to their varying structure, they offer different advantages (Figure 2). IER bags are a collection of resin beads, providing resin bags with a higher resin surface area, and thus larger ionic holding capacity (Meason & Idol, 2008). However, quantifying the surface area available

in an IER bag is difficult individual resin beads at the center of a resin bag may contact only one another rather than contributing to the surface area of resin in contact with soil. IEMs have a simpler structure with two flat surfaces of resin, allowing for easy quantification of resin surface area, but more limited ionic holding capacity (Meason & Idol, 2008). Data comparison between IEMs and IERs is difficult because of varying units, where IEMs measure mass ion absorbance per surface area and IERs report mass absorbed per mass resin.

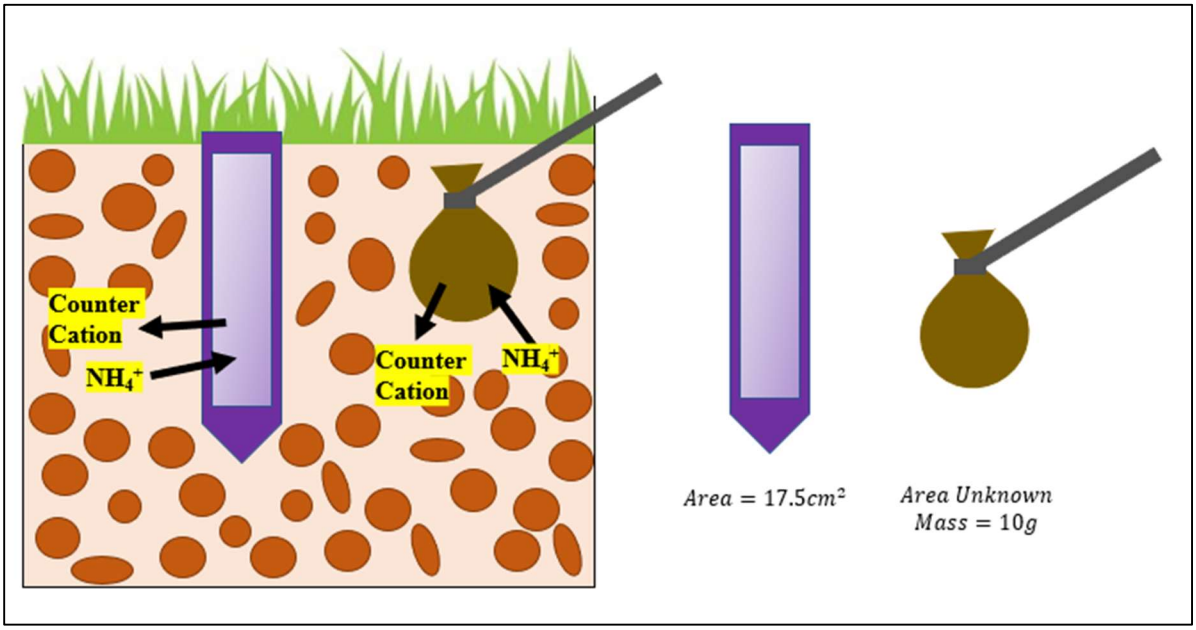

Figure 2: Comparison of in-situ IER tools. IER membranes (purple, left) were installed vertically, and have a known surface area. IER bags (brown, right) were composed of sand-like IER beads with an unknown surface area and known IER mass.

Validity of measurements with IERs has been tested under varying burial lengths, soil moisture regimes, extraction procedures, and with varying burial orientation. Burial

periods for IERs range from burst-measurements (1 hour for resin beads, to 1 day for resin membranes) to 6 month-long burials (for beads) (Meason & Idol, 2008). Varying burial lengths require different conceptual analysis, as burst measurements will not reflect equilibration with soil demands, and this could be a major contributor to month-long measurements (Meason & Idol, 2008; Qian & Schoenau, 2002). Soil moisture influences the measurement of available ions as higher soil moisture is associated with the creation of pore-space connections, providing pathways for ions through soil to IERs (Pampolino & Hatano, 2000; Qian & Schoenau, 2002). This, however, is the same relationship that hinders nutrient transport in soils (to plants or out of soils), and it is therefore conceptually desired when analyzing nutrient availability (Qian & Schoenau, 2002). IER measurements can also vary depending on the eluent used to strip collected soil ions off the IER. In this process, IERs are soaked in a counter-ion solution to detached the measured ions, where ionic strength of the counter ion must be considered (Qian & Schoenau, 2002). The final consideration for IER use is the orientation of IERs in soil. This variability is relevant particularly for IEMs, as the alignment of the membrane surface area as perpendicular or parallel to predominant soil flow paths has the potential to impact the mobility of ions. It has been found that IEM burial orientation had little influence on nutrients like P and potassium, but can be influential on readings of manganese and iron (Bremer, Miller, & Curtis, 2018).

IEMs have been applied in ecological (Bremer et al., 2018; Langenhove et al., 2020; J. J. Miller, Bremer, & Curtis, 2016; Norby, Sloan, Iversen, & Childs, 2019), agricultural (Martinsen et al., 2014; Qian & Schoenau, 2007; Sharifi, Lynch, Zebarth, Zheng, & Martin, 2009), and forestry (Collin, Messier, & Belanger, 2017; Harrison &

Maynard, 2014; Switzer, Hope, Grayston, & Prescott, 2012) research to measure nutrient supply rates. Despite extensive use in many sectors of biogeoscience research, no cases of IER or IEM use in GSI are known. This research employs IERs and IEMs to monitor available nutrients in various urban green spaces.

Reviewing literature resulted in the identification of gaps in knowledge of seasonality of nutrient availability in urban green spaces. Previous seasonality studies had contradicting results and mixed understanding of the influence of seasonality on mechanisms that control nutrient availability. This literature review also provided support that IERs and IEMs would be suitable tools for monitoring available nutrients in urban soils. Building upon foundational knowledge discussed in this literature review, it was hypothesized that 1) nutrient availability would vary with season, and 2) seasonal changes in environmental drivers would affect the seasonality of nutrient availability.

3. METHODS

3.1 Experimental Design

The masses of available nitrate, ammonium, and phosphate were monitored for 24 weeks during the 2019 growing season, in three urban green spaces: 2 urban garden beds, a greenroof, and a constructed stormwater wetland (in upland and lowland positions). Observations of nutrient availability were broken into 12 two-week periods henceforth called observation intervals. The three field sites had staggered observation intervals, where observations began April 15, 2019 at the urban garden beds, April 18, 2019 at the green roof, and April 24, 2019 at the constructed stormwater wetland. Concurrent observations of five environmental drivers were made at all three sites. Seasonal variability in nutrient availability and seasonal variability of environmental drivers were observed simultaneously.

The various sites studied were all located in Milwaukee, WI and defined by varying drainage areas and surface cover. The urban garden plots were elevated garden beds planted with common garden vegetables and herbs and receiving no stormwater beyond direct precipitation (Figure 3). There was no design difference between the two garden plots, labeled as West plot and East plot, but garden plant species differed between the two plots. Green roof cover consisted of sedums, and the roof received no downspout connections, so that the drainage area was equal to the surface area (Figure 4). The constructed stormwater wetland consisted of an upland plot and lowland plot where the upland was sloped, and the lowland was flat and inundated with water following precipitation events. Both wetland locations were heavily vegetated with reeds,

wildflowers, tall grasses, and scattered trees (Figure 5). The drainage area of the upland plot was surface area, but the lowland was a drainage point for the neighboring industrial park.

Figure 3: Urban garden plots located on Marquette University campus in Milwaukee, WI. The plots were monitored separately and named West plot (left) and East plot (right).

Figure 4: A greenroof on Engineering Hall on Marquette University campus, Milwaukee WI.

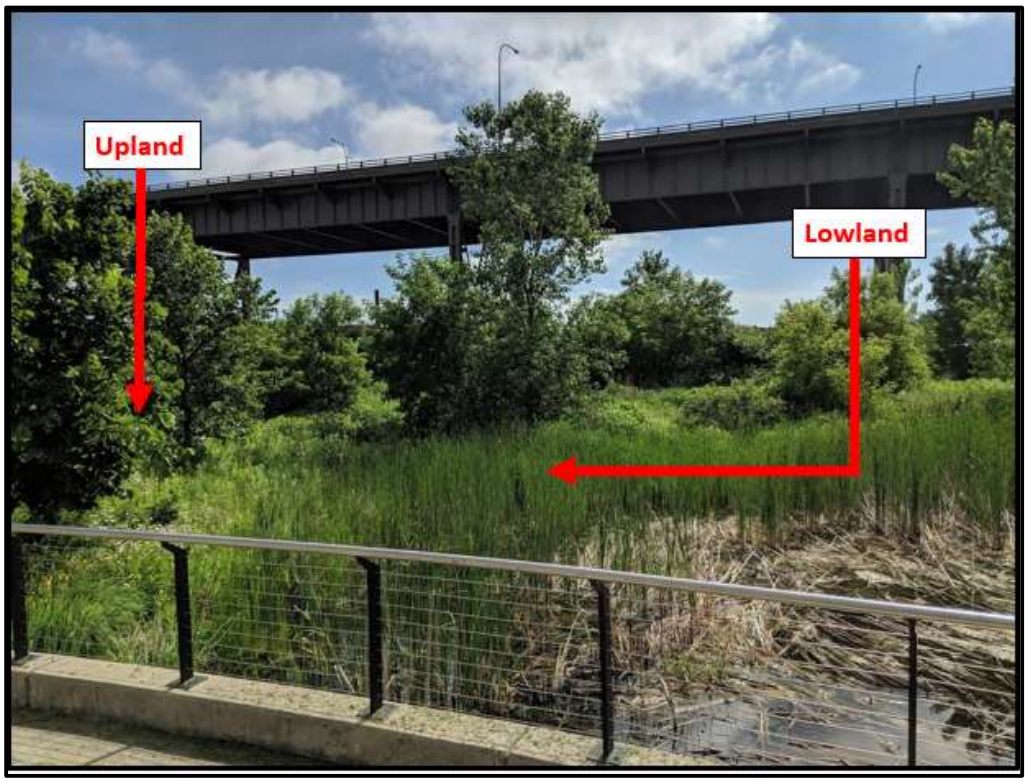

Figure 5: A constructed stormwater wetland at an industrial park on 35th St in Milwaukee WI. The wetland consisted of two sub-plots, an upland that was sloped lowland area at the edge of the pond's permanent pool than became submerged with water following precipitation events.

3.2 Environmental Drivers

Environmental drivers observed were air temperature (T_A), precipitation (P), time, soil temperature (T_S), volumetric water content (VWC), and soil oxygen (O_2). These drivers are conceptually grouped into two categories: hydroclimatic drivers T_A, P, T_S, VWC, and biogeochemical indicator O_2. An additional variable, time, is also considered as a measure of increasing or decreasing over time. Hydroclimatic drivers indicate how climate, and or hydrology impact the soil and the biogeochemical indicator provides a proxy of biogeochemical aerobic activity. Environmental driver data was either obtained from in-situ data loggers at each site (T_S, VWC, O_2) or from a local weather station (T_A, P). All data was collected at either a 5-minute (auto logger obtained) or daily (weather station) frequency, then averaged into two week-long intervals, to match the observation intervals used for nutrient monitoring.

In-situ environmental drivers were measured with automatically logging sensors at a five-minute collection interval. Soil oxygen and soil temperature were recorded with Apogee SO-110 sensors (accuracy ±0.1%, 1mV drift per year), and soil moisture with Campbell Scientific CS650 water content reflectometers (±3% accuracy). All sensors were buried 15cm below the soil surface. Soil oxygen sensors at the wetland were housed within PVC cylinder enclosures to minimize sensor clogging under saturated conditions. All in-situ measurements had staggered start-dates as monitoring equipment was installed in phases. In-situ garden plot monitoring began prior to the scope of this project, resulting in data observations for all twelve observation intervals. Measurements at the constructed wetland began on May 18, 2019. As a result, the first two-week averages at the wetland could not be calculated until the third wetland nutrient

observation, May 22 to June 5, so that a total of 10 two-week average in-situ environmental driver points were observed (Appendix Tables A4 and A5 at the Wetland Upland and Lowland, respectively). Green roof sensors were installed on June 13, 2019, where the first four collection intervals were missed, to result in 8 total overlapping two-week average observations of green roof nutrient availability and in-situ soil data (Appendix Table A3).

Observations of the hydroclimatic drivers precipitation and air temperature were obtained from Climate Data Online run by the National Oceanic and Atmospheric Administration, where weather was retrieved for the weather station at the General Mitchell Airport in Milwaukee, WI (Station ID WBAN:14839). Data was retrieved as a daily temperature average (distinguished from soil temperature as "air temperature") and cumulative daily precipitation. Station data was monitored from April to October 2019. Daily air temperature averages and daily precipitation accumulations were averaged to two-week average temperature, and cumulative two-week precipitation, structured to parallel the observation intervals observed at each of the three sites. Daily data is the same for all sites because the same weather station was used for all sites, but two - week averages vary between sites, as these averages reflect the various nutrient observation intervals at each site. Subplots of the same site (i.e. upland and lowland of the constructed stormwater wetland and West plot and East plot of the urban gardens) have identical precipitation and air temperature data because they have the same observation interval.

3.3 Nutrient Availability

Nitrate, ammonium, and phosphate were monitored with both IER bags and IEM. Both resin monitoring tools were separated into anion-collecting (anion) and cation-

collecting (cation) resins. These resins measure the availability of nutrients in soil, a function of the quantity of labile nutrients and the mobility of those nutrients. Availability, in the context of this project is used to describe the net amount of nutrients that are both labile and mobile minus cumulative soil system nutrient demands. In this work, labile nutrients are considered those nutrients free in the soil media (not otherwise used by a soil biogeochemical binding mechanism). Mobile nutrients are defined as those nutrients able to traverse the soil to reach IERs via either diffusion or bulk transport in pore water. A nutrient ion must be both labile and mobile to be measured by IER and IEM monitoring tools. Thus, nutrient observations are not measurements of the concentration of ions in soil pore water, but the detection of those ions, which is dependent on soil pore water ion concentration and the transport mechanism. These detectable soil pore ions are a proxy of those ions susceptible to leaching from the soil system in effluent. This conceptual model assumes that the bulk system concentration, or total available nutrients in the soil systems, is equivalent to the effluent concentration, or monitored available nutrients, like in a continuous stirred tank reactor. Through this logic, nutrients measured by IERs are representative of the quantity of nutrients present in the soil system that are susceptible to leaching and transport by stormwater to receiving waters.

3.3.1 IER Bags

IER bags were both constructed and analyzed in-house. Anion and cation IER beads were Dowex 1-X8 (chloride form 50-100 mesh) and Dowex 50WX8 (hydrogen form, 50-100 mesh), respectively (Bailey Boomer & Bedford, 2008; Y. Lundell, 1989; Ylva Lundell, 2001). To construct the IER bags, 10g of resin were placed in the center of

a 100 cm^2 square of nylon cut from commercially available pantyhose (Billings, Schaeffer, & Evans, 2004; Krause & Ramlal, 1987; Lajtha, 1988; E. M. Miller & Seastedt, 2009). Resin bags were cinched closed with zip ties and color-coded to identify the different IER forms (Krause & Ramlal, 1987). Cation bags were maintained in hydrogen form, while anion bags were converted to bicarbonate form as an easily exchanged counter-ion (Bailey Boomer & Bedford, 2008; Krause & Ramlal, 1987; Qian & Schoenau, 2002). Anion bags were charged with bicarbonate by soaking the anion resins in 0.5M $NaHCO_3$ for 1 hour. All resin bags were rinsed in nano-pure deionized (DI) water. After this pretreatment process, resin bags were kept in plastic resealable bags and stored in a refrigerator.

IER bags were transported to the field in a cooler. In the field, the IER bags were buried by creating a 10cm long slit in the soil with a trowel, at approximately a 45° angle. The bags were inserted into this soil wedge, and the soil flap was then pressed back down and compressed gently to ensure contact with the resin bag. Exactly 14 days after deployment, bags were retrieved by lifting the soil flap made during deployment and removing the bags from below with a trowel. IERs were then bagged in plastic resealable bags and transported to the lab in a cooler where they were rinsed in DI water and extracted within 2 hours.

Nutrient ions from cation and anion bags were extracted by stirring the DI-rinsed IER bag in 100mL of eluent on a stir plate at 175 rpm for one hour, where cation bag eluent was 1M HCl, and anion bag eluent was 1M NaCl (Giesler, Morth, Mellqvist, & Torssander, 2005; Y. Lundell, 1989; Ylva Lundell, 2001; Qian & Schoenau, 2007). The eluted extract was then filtered in a gravity filter with 100nm glass fiber filter paper.

Samples were bottled in 50mL plastic storage vials and stored in a refrigerator until analysis. Cation samples were tested for ammonium (Weatherburn, 1967). Anion samples were tested for nitrate (Doane & Horwath, 2003) and phosphate (Lajtha, Driscoll, Jarrell, & Elliott, 1999). Filtered eluent samples were analyzed for nutrients using colorimetric methods, measured on a VERSAmax turntable microplate reader spectrophotometer (Molecular Devices, San Jose CA). Colorimetric results were measured as a concentration (ppm). Concentration units were converted to mass by considering the volume of eluent used during extraction (100mL). Final nutrient availability data units are conceptually defined as mass of constituent per mass of resin in an IER bag, per burial period (units of μg nutrient · 5g resin^{-1} · 2-weeks^{-1}) and labeled subsequently as μg of available nutrient ion as resin mass and burial length were uniform for the study.

Checks for accumulated ion carry-over were done every week to monitor the performance of the IER bags over the course of the study period. This was accomplished by designating one cleaned IER bag previously used in the field to be left unburied over the course of a two-week observation interval. These unburied bags were termed "blanks" as they were not buried in the soil, and therefore should not accumulate any ions. During the first four observation intervals one blank was shared for all sites, then for all subsequent observation one blank was analyzed per site, per observation interval. Blanks were extracted and analyzed with identical methods used on the buried IER bags. Through blanks analysis, accumulation of nutrients on IER bags from use-to-use was monitored.

3.3.2 IEM

The IEMs used were the commercially available Plant Root Simulator (PRS) probes from Western Ag Innovations (Saskatoon, SK, Canada). The probes consist of a plastic encasing around two 55mm x 16mm IEM surfaces for a combined front-and-back contact surface area of 17.5 cm^2. Maximum adsorption capacity was 208.6 $\mu g/cm^2$, 331.8 $\mu g/cm^2$ and > 231.0 $\mu g/cm^2$ for nitrate, ammonium, and phosphate, respectively ("PRS Technology," 2020).

PRS probes were buried in pairs: one cation-collecting and one anion-collecting probe. Three pairs were buried at both plots for each collection interval. Cation and anion pairs were buried between 2 and 5ft apart. At the constructed stormwater wetland upland where elevation was relevant, IEMs were placed along the same approximate contour. Probes were buried vertically at depths ranging from 5 to 12 cm along the IEM surface, and further burial procedures were conducted in accordance with direction from Western Ag Innovations. Probes were buried for 2-week intervals (exactly 14 days). Following each collection interval, probes were retrieved in accordance with Western Ag protocol. Placement of probes were flagged in the field to avoid repeat burial location to minimize the influence of soil disturbance on data. After retrieval, PRS probes were packaged into resealable plastic bags and transported to the lab in a cooler, where they were rinsed with DI water and sealed into new plastic bags and stored in a refrigerator. Samples were sent to Western Ag Innovations Inc. (US lab Moscow, ID) for analysis. Ion extraction was performed with counter ion Na^+ for cation probes and HCO_3^- for anion probes. Nitrate and ammonium were analyzed colorimetrically via flow injection analysis (Skalar San++

Analyzer, Skalar Inc., Netherlands). P was analyzed with inductively coupled plasma (ICP) spectrometry (Optima ICP-OES 8300, PerkinElmer Inc., USA). While ICP analysis includes all P forms, only ionic P is mobile in soil and able to be absorbed by IEMs (Bremer et al., 2018).

3.4 Statistical Analysis

Multiple linear regression was performed to determine which explanatory variables significantly contributed to the variation in nutrient availability. For each nutrient, explanatory variables considered were hydroclimatic variables (T_A, P, T_S, VWC), biogeochemical indicator O_2, time, and the availability of the other nutrients. Unpaired samples of nutrient availability and explanatory variables were excluded. Model selection used the backwards selection method (with F-test) to identify the model with the highest explanatory power.

Collinearity and skewness were checked for all explanatory variables at all sites. Each independent variable was tested for skewness to show variation from a normal distribution and collinearity was investigated to identify any interdependencies between independent variables. Skewness values > 1 and < -1 were considered highly skewed. Pairs of independent variables were determined to be collinear if the collinearity between them (R^2) was greater than 0.1.

4. RESULTS

4.1 Seasonality Observations with IER Bags

Ion carry-over was observed with the IER bags, and therefore IER bag data was not reliable and was not included in the results or discussion of this work. Blank IER bags should have had no or low detectable ions as they were not buried in the field before extraction. However, after 3 to 5 observation intervals blanks showed significant extracted ions (Figure 6,7,8). This indicated that there was ion carry-over from a previous use of the IER bag in the field. Therefore, the extraction process did not reliably strip all ions off IER bags.

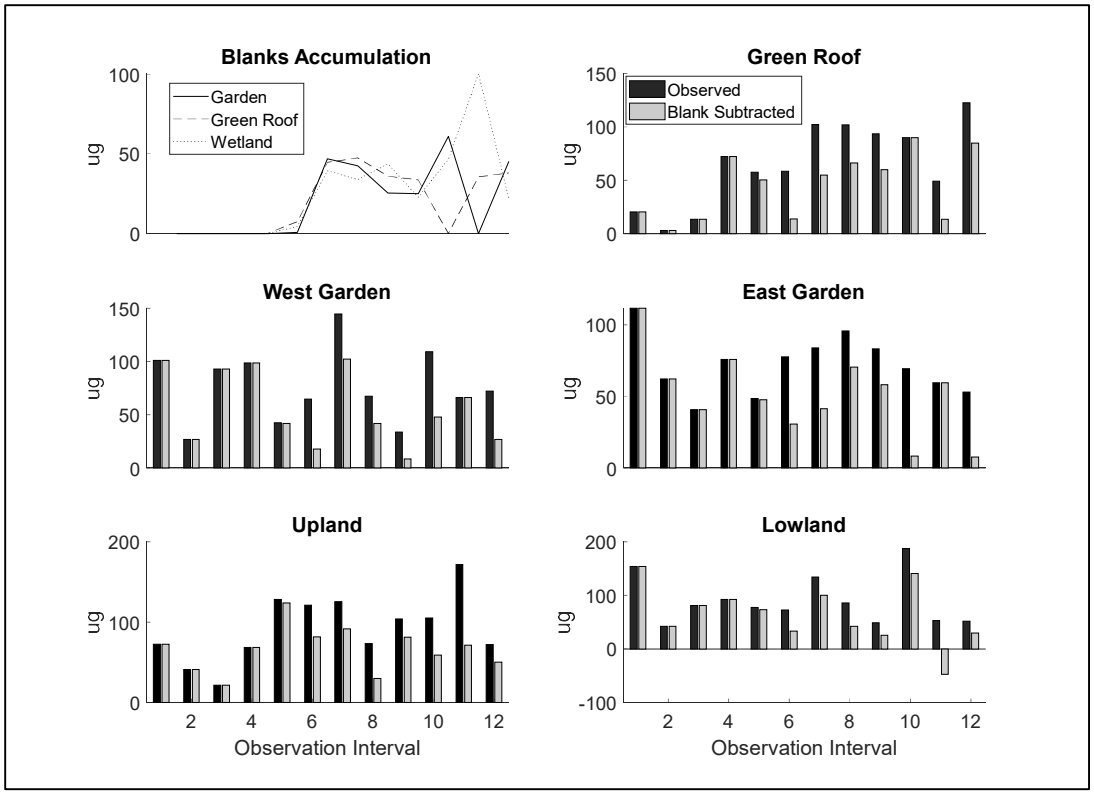

Figure 6: Analysis of ammonium accumulation on IER bag blanks. Timeseries of ammonium accumulation on IER bag blanks and difference between observed values of nitrate availability compared to nitrate observation with blank values subtracted at the green roof, West garden, East garden, upland and lowland plots of the constructed stormwater wetland.

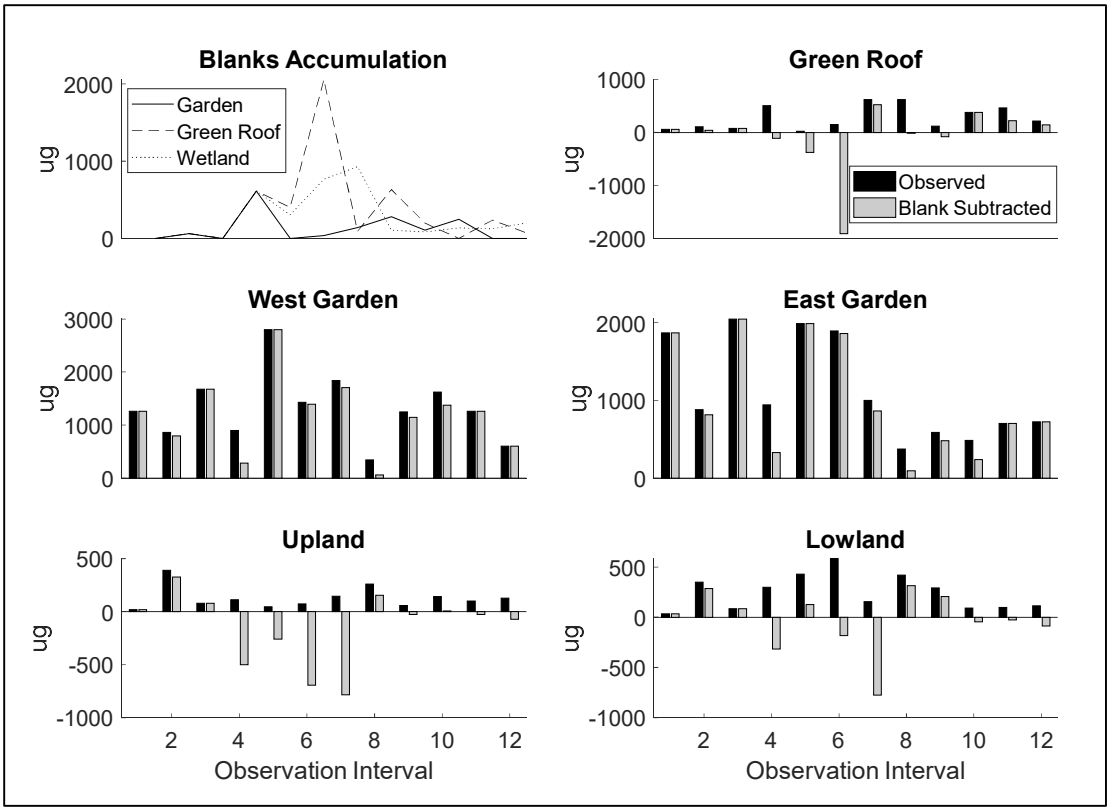

Figure 7: Analysis of nitrate accumulation on IER bag blanks. Timeseries of nitrate accumulation on blanks and difference between observed values of nitrate availability compared to nitrate observation with blank values subtracted at the green roof, West garden, East garden, upland and lowland plots of the constructed stormwater wetland.

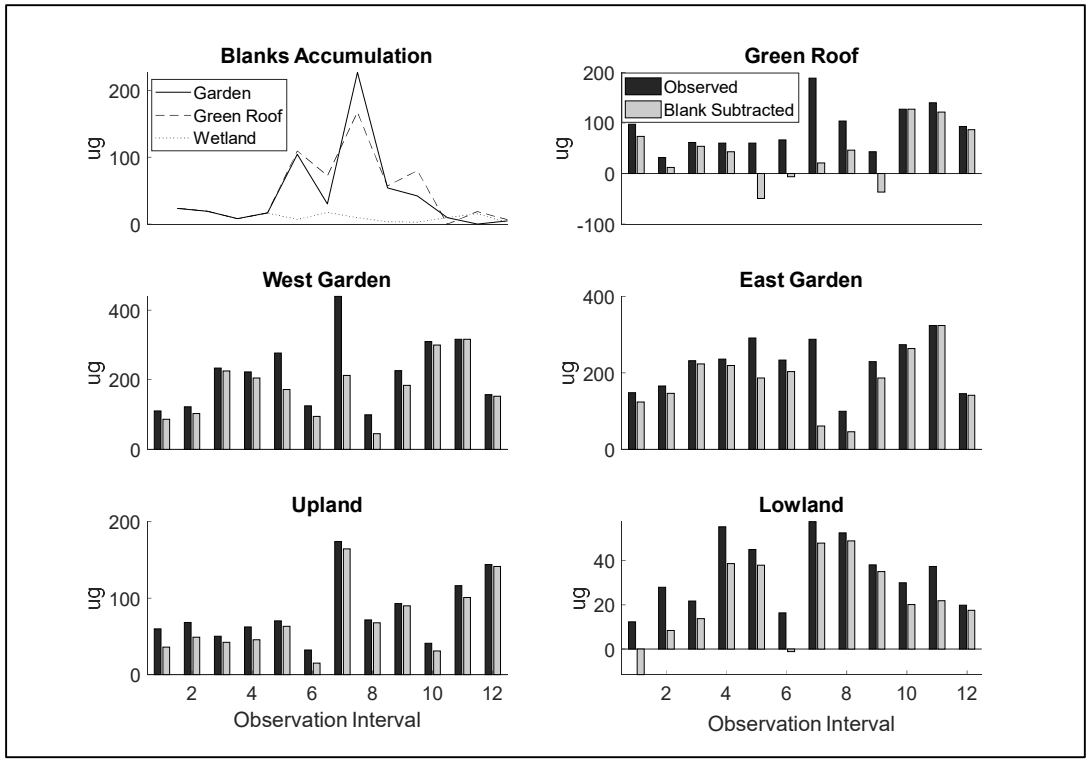

Figure 8: Analysis of phosphate accumulation on IER bag blanks. Timeseries of phosphate accumulation on blanks and difference between observed values of nitrate availability compared to nitrate observation with blank values subtracted at the green roof, West garden, East garden, upland and lowland plots of the constructed stormwater wetland.

Blanks analysis showed all nutrients to have non-zero detection on blanks for most (>6) observation intervals. Nitrate was the most abundant nutrient to be found on blanks (Figure 7). Ammonium and phosphate were both also found on blanks, but to a lesser degree (Figure 6,Figure 8). The impact of incomplete nitrate extraction is shown in Figure 7, where all blanks after the fourth observation interval showed nitrate accumulation had occurred. Nitrate accumulation had the largest impact on green roof and wetland data. Garden nitrate availability was so large that the error introduced from accumulation on blanks was minimal compared to observed availability. Overall analysis of blanks showed incomplete extraction was performed in the analysis of IER bags,

making IER bag data unreliable as a measure of total available nutrients. IER bag data is not included in the results of this study and henceforth discussed for only for methods improvement and not quantitative analysis.

4.2 Historical Context of Environmental Variability

Monthly precipitation and temperature data collected during the study period were compared to the 2010 NOAA thirty-year monthly normals (Table 1). Monthly average temperatures were cooler in May and June and warmer than average in July through September. Average daily temperature during the study period ranged from 39°F to 84°F on April 15 and July 19, respectively. The study period was wetter than the thirty-year monthly normal in shoulder months (April, May, June, September, and October), and drier than average in July and August. The shoulder seasons were defined by frequent, low-intensity precipitation, whereas precipitation was infrequent and intense in summer months (Sharior, McDonald, & Parolari, 2019).

Table 1: Monthly observed cumulative precipitation compared to 30-year monthly normals. Average temperature during the study period (April-October 2019) compared to NOAA 30-year monthly normals (1981-2010).

		April	*May*	*June*	*July*	*August*	*September*	*October*
Cumulative Monthly Precipitation (In.)	2019	3.77	6.32	4.42	3.17	3.53	7.00	6.48
	1981-2010	3.56	3.40	3.90	3.67	3.97	3.18	2.65
Average Temperature (F)	2019	46.5	53.6	63.4	75.1	71.8	67.5	50.4
	1981-2010	45.6	55.7	66.2	71.8	70.7	63.1	51.3

4.3 Statistical Checks

4.3.1 Skewness

The only skewed variable was soil oxygen, which was found to be skewed at the East garden, green roof, and wetland upland. At each of these locations, soil oxygen was negatively skewed, with the strongest negative skew at the upland plot of the wetland (Table 2). Strong negative skewness indicates that the soil oxygen data tended to have more high-oxygen observations with some low oxygen observations, driving a left-tail.

Table 2: Measures of skewness for each independent variable at all study sites.

Location	Time	Precipitation	VWC	T_A	T_S	O_2
West Garden	0.00	0.84	0.14	-0.58	-0.52	0.13
East Garden	0.00	0.84	0.02	-0.58	-0.85	-1.65
Green Roof	0.00	0.59	-0.02	-0.58	-0.16	1.06
Wetland Upland	0.00	-0.27	-0.14	-0.75	-0.15	-2.03
Wetland Lowland	0.00	-0.27	-0.64	-0.75	0.10	-0.63

4.3.2 Collinearity

Relationships between environmental drivers varied depending on site location. Two sets of environmental drivers were strongly correlated at all sites: air temperature and soil temperature, and air temperature and volumetric water content. The coefficient of determination between soil and air temperature was the highest correlated collinear relationship at all sites, where coefficients of determination ranged from 0.94 at the wetland lowland to 0.99 at the green roof. Correlations between volumetric water content and air temperature were more moderate, with coefficients of determination ranging from

0.17 at the wetland lowland to 0.74 at the West garden. All statistical parameters determined in collinearity evaluations are reported in Tables A 12- A16 in the Appendix.

4.4 Relationship between VWC and O_2

In general, O_2 decreased with VWC. The relationship between VWC and O_2 varied between sites, where the lowland profile was the most distinct due to the consistently high VWC. The green roof consistently had the lowest VWC and highest O_2. The West plot and wetland upland displayed similar traits, with high O_2 regardless of changes in VWC, and the East plot showed a similar trend at lower O_2 levels. Converse to the other sites, the lowland had highly varying O_2 within a narrow VWC range. Across all sites, as VWC increased, O_2 decreased in a non-linear fashion. Below a VWC of 40%, O_2 gradually decreased with decreasing VWC, while above this threshold, O_2 decreased rapidly as soils approached saturation (Figure 9).

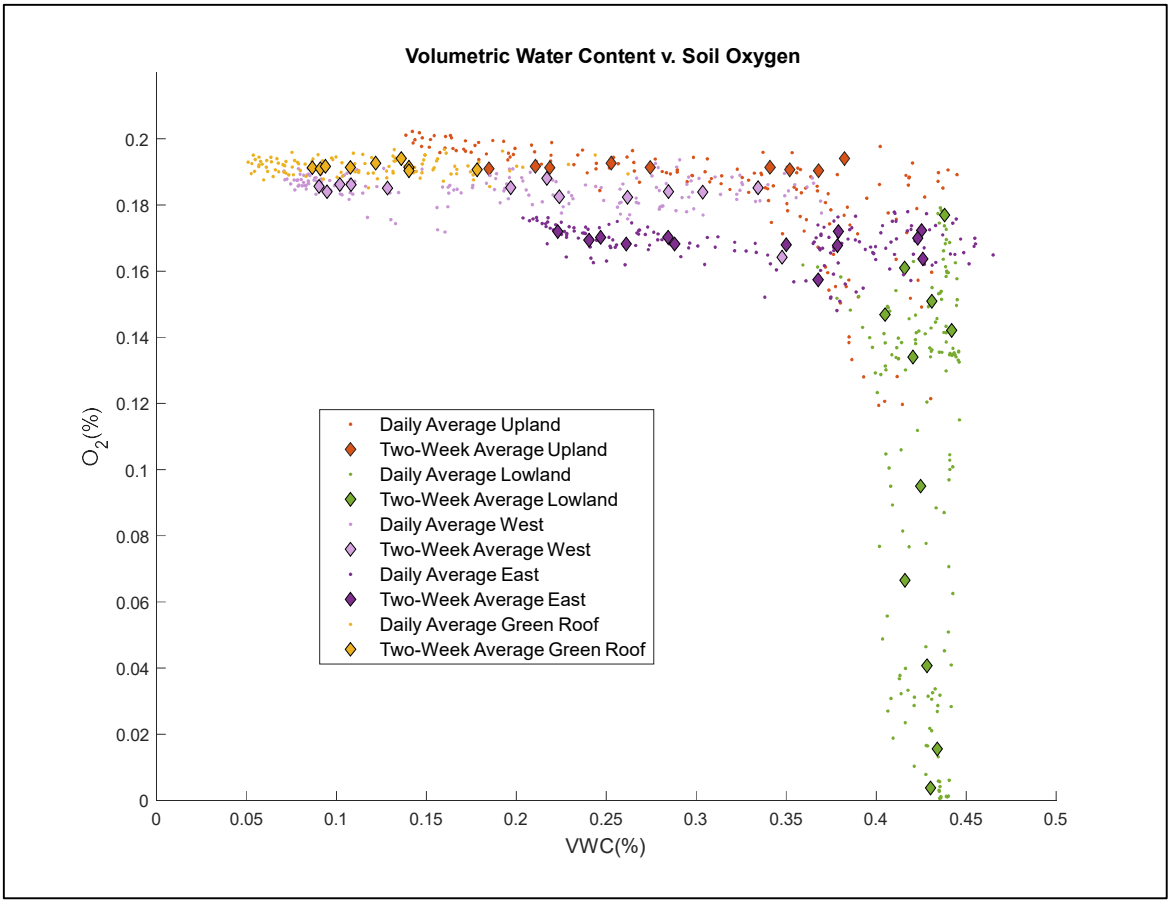

Figure 9: Soil oxygen response to soil moisture at all observed locations. Points show average daily observations, and diamonds show two-week average observations.

4.5 Urban Gardens

4.5.1 Environmental Drivers

Environmental drivers at the West and East plots were very similar, displaying parallel observations in soil moisture, soil oxygen, and soil temperature at slightly altered levels from one another. Precipitation was highest at the gardens during the interval from September 2 to September 6, during which 5.1 in of precipitation fell. However, VWC at the garden was higher in the spring and early summer, decreasing to lower levels in mid-July where it remained low until more frequent precipitation in September. The East plot

had a consistently higher VWC than the West plot (Figure 10). Conversely, soil oxygen was consistently higher in the West than East plot. Seasonality of soil oxygen was consistent- confined to 1% change at both gardens (East garden range 16-17%, West garden range 18-19%). Soil temperature was nearly identical for the garden plots, briefly diverging in the highest summer temperature readings, as East garden soil temperatures were higher (Figure 10).

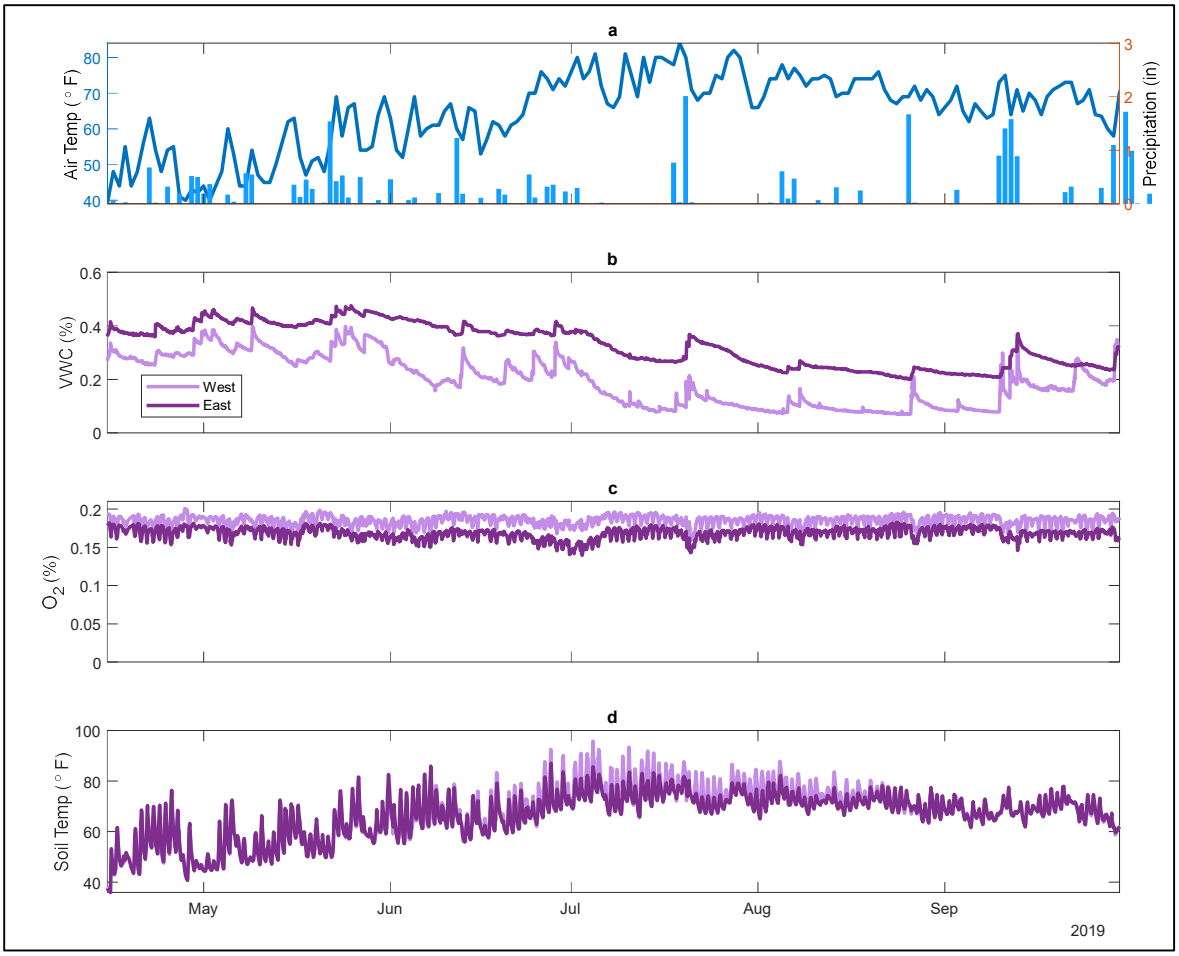

Figure 10: Seasonal variability in environmental drivers at the urban gardens. Precipitation (a), air temperature (a), soil moisture (b), soil oxygen (c), and soil temperature (d). In-situ soil data was recorded at both the West (dark purple) and East garden (light purple). In-situ soil data are plotted at a 5-minute frequency, temperature is plotted as a daily average, and precipitation is plotted as a daily total.

4.5.2 Seasonality of Nutrient Availability

Nitrate was the most available nutrient at both the garden plots (Figure 11). Average availability of nitrate was 294 µg ± 171 in the West garden plot and 304 µg ± 216 in the East. There was no significant difference in nitrate observations between the two plots. Nitrate was the most available N-species monitored, exceeding the availability of ammonium by 65 and 57 times in the West and East gardens, respectively. Nitrate was

also 8 times more available than phosphate in both gardens. Intra-site variability of nitrate was high over the course of the study, where the lowest garden observation was 46 µg (in the East Garden from August 19- September 2), and the highest observation was 704 µg (in the East garden from April 15 – April 29). After a high first observation in late April, a seasonal pattern in nitrate was observed, where nitrate increased from early May to a peak in late June, followed by a decrease through early August (Figure 11). Following the early-summer peak, nitrate stabilized at around 200 µg of available nitrate per two-week observation interval from early August until the end of the study period in late September.

Ammonium was the least available of the three observed nutrients at both garden plots. Average ammonium availability was 4.5 µg ± 3.4 in the West plot and 5.3 µg ± 3.6 in the East plot. Four of twelve ammonium observations were below the observation limits in the West plot (April 15- April 29, May 13- May 27, May 27- June 10, and July 22 – August 5), and two were below the detection limit in the East plot (April 15 – April 29, and May 27 – June 10) (Figure 11). Ammonium was undetectable (no measured available ions) in both garden plots from May 27 to June 10. In general, ammonium was more available in late summer and early fall than in spring and early summer (Figure 11).

Phosphate was the second most available nutrient in both garden plots and displayed little apparent seasonality. Average phosphate availability was 35.8 µg ± 11.8 in the West and 36.4 µg ± 13.5 in the East. Observations ranged from a minimum of 17.4 µg to maximum 58.1 µg, both occurring in the East plot. Phosphate had no clear seasonal pattern or distinct high pulses in either garden (Figure 11).

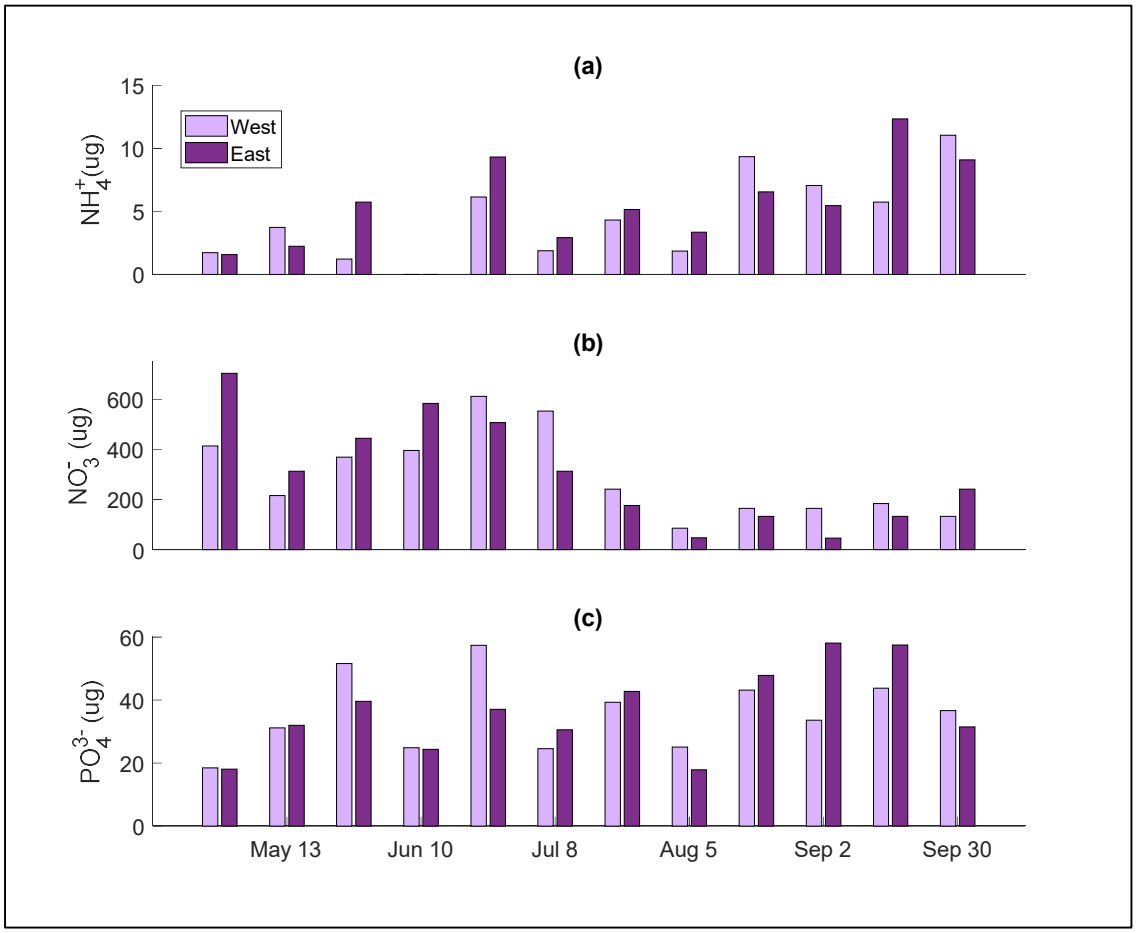

Figure 11: Seasonality of nutrients at the urban gardens. Ammonium (a), nitrate (b), and phosphate (c) are plotted as measured with IEMs over the duration of the green roof study period, from April 15 to September 30. Ammonium was non-detect at both gardens for the fourth observation interval, May 27 to June 10.

4.5.3 Regression Analysis

Models estimating nutrient variability were selected for all three nutrients in both gardens. Time and precipitation were the most common explanatory variables for nutrients at the urban garden plots (Table 3). Garden nutrient availability model predictions are compared to observed data in Figure 12.

In the West plot, N species were strongly associated with time, and phosphate variation was associated with precipitation and oxygen. Forty-seven percent of ammonium availability in the West plot was positively associated with time ($p = 0.00$,Table 3), indicating higher ammonium availability in late summer and fall than in spring and early summer. Conversely, nitrate was negatively associated with time, which was responsible for 26.9% of variability ($p – 0.005$,Table 3) and therefore was most available earliest in the study period and declined in availability over time. Phosphate in the West plot was positively associated with both precipitation and oxygen, which together explained 44.6% of variability in phosphate ($R^2 = 0.4457$ $p = 0.02$,Table 3).

All three nutrients in the East plot were best modeled by different two-variable models. East plot ammonium was positively associated with both time and precipitation so that ammonium was most available in wet observation intervals in late summer and early fall. The best significant explanatory variables for nitrate were air temperature and soil oxygen content, indicating that nitrate was most available during well oxygenated times in the summer. East plot phosphate was positively associated with precipitation, but negatively associated with VWC, together explaining 62.2% of phosphate variability.

In both garden plots, ammonium was associated with time, nitrate was associated with either time or temperature, and phosphate positively related to precipitation. Ammonium availability was seasonal, with increasing availability over the growing season. Nitrate availability increased from spring to summer or was highest during highest temperature intervals. Finally, phosphate availability was not seasonally dynamic, but rather most influenced by high precipitation.

Table 3: Statistical Parameter from multiple linear regression analysis in the urban gardens. Linear regression model coefficients, coefficient of determination (R^2) and p value significance tester are shown for each model.

Nutrient	Time	Precipitation	VWC	T_A	T_S	O_2	Adj. R^2	p
West								
NH_4^+	0.7240	-	-	-	-	-	0.4771	0.0077
NO_3^-	-0.5789	-	-	-	-	-	0.2687	0.0486
PO_4^{3-}	-	0.5480	-	-	-	0.4610	0.4457	0.0285
East								
NH_4^+	0.6246	0.5470	-	-	-	-	0.6753	0.0026
NO_3^-	-	-	-	-0.9020	-	-0.5006	0.6757	0.0026
PO_4^{3-}	-	0.6140	-0.5750	-	-	-	0.6223	0.0051

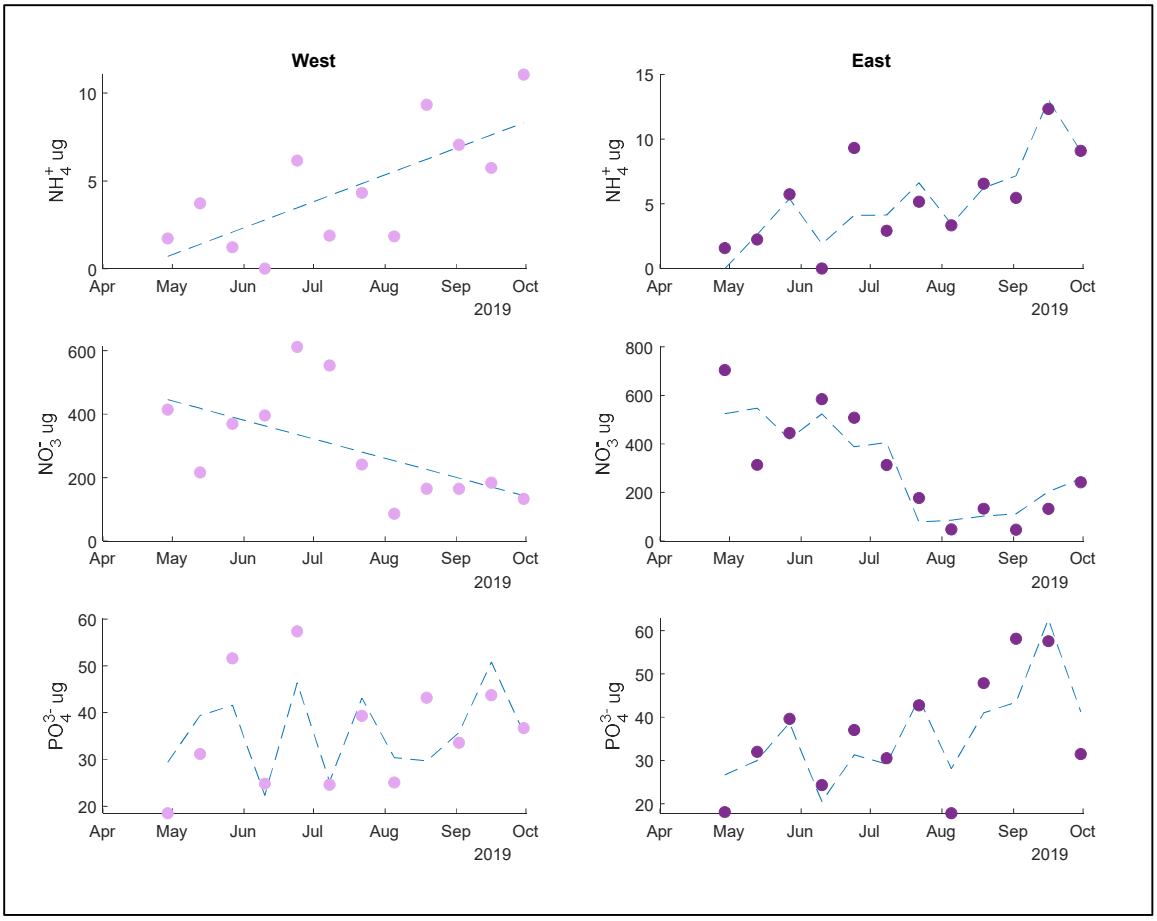

Figure 12: Multiple linear regression model results plotted against observed nutrient availability at the urban gardens. Left columns show the model performance for the West garden and right columns show model performance at the east garden where ammonium, nitrate, and phosphate models are shown (top to bottom).

4.6 Green Roof

4.6.1 Environmental Drivers

The green roof was defined by flashy volumetric water content, and low variability in soil oxygen. Precipitation was highest at the green roof during the last two observation intervals spanning September 5 to October 3, in which cumulative two-week precipitation was 4.8 in and 4.7 in, respectively. During these two highest precipitation accumulations, as well as for earlier precipitation events, volumetric water content both

rose and fell quickly in response to rainfall events (Figure 13). However, soil oxygen was consistent over the timeseries, remaining at 19% for the duration of the study period, almost 2% lower than atmospheric oxygen.

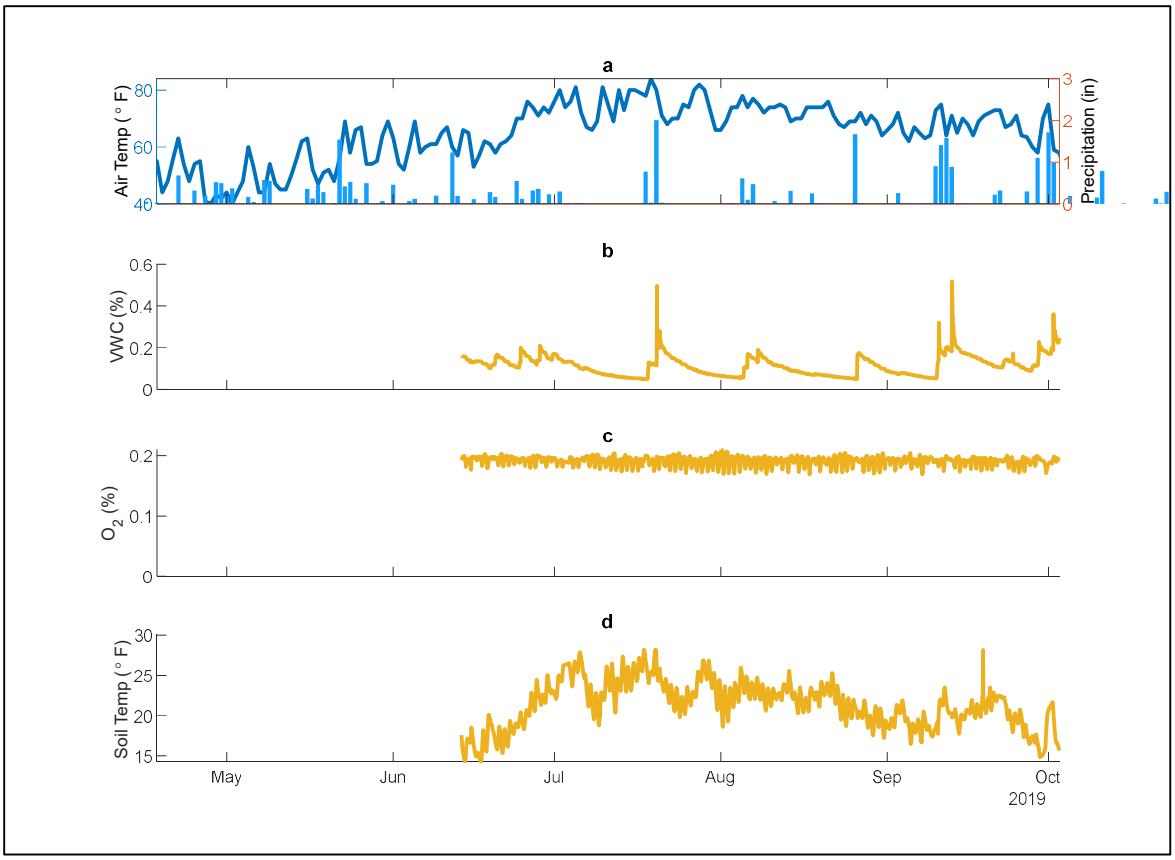

Figure 13: Seasonal variability in environmental drivers at the Green Roof. Precipitation (a), air temperature (a), soil moisture (b), soil oxygen (c), and soil temperature (d). In-situ soil data are plotted at a 5-minute frequency, temperature is plotted as a daily average, and precipitation is plotted as a daily total.

4.6.2 Seasonality of Nutrient Availability

Nitrate was the most abundant nutrient at the greenroof, with nitrate availability comparable to availability at the constructed stormwater wetland, and much lower than at

the garden plots (average availability 14.0 µg ± 6.9). Nitrate ranged in availability from 4.5 µg available from June 13 - June 27, to 28.3 µg available September 19 – October 3. In general, nitrate availability was lower in the spring and early summer (9.7 µg) than in the fall and early winter (18.3 µg) (Figure 14).

Ammonium was least available of the nutrients at the green roof. Ammonium availability averaged 4.9 µg ± 3.0 over the study period and peaked during the second observation interval from May 2 -May 16, (10.8 µg). Ammonium was below detection limit for one observation, from May 30 – June 13. There was no clear seasonal trend in ammonium at the green roof (Figure 14).

Phosphate availability was between nitrate and ammonium availability, and it showed no clear seasonal change. Average availability of phosphate was 7.6 µg ± 4.5, and phosphate ranged from a minimum of 2.7 µg from July 25 – August 8 to maximum availability of 18.8 µg from September 19 to October 3, the same observation interval with the highest nitrate pulse. Phosphate had occasional high availability pulses in the spring and summer surrounded by otherwise low availability and increased through the fall as seen by increasing availability from August 8-August 22 through the end of the study period (Figure 14).

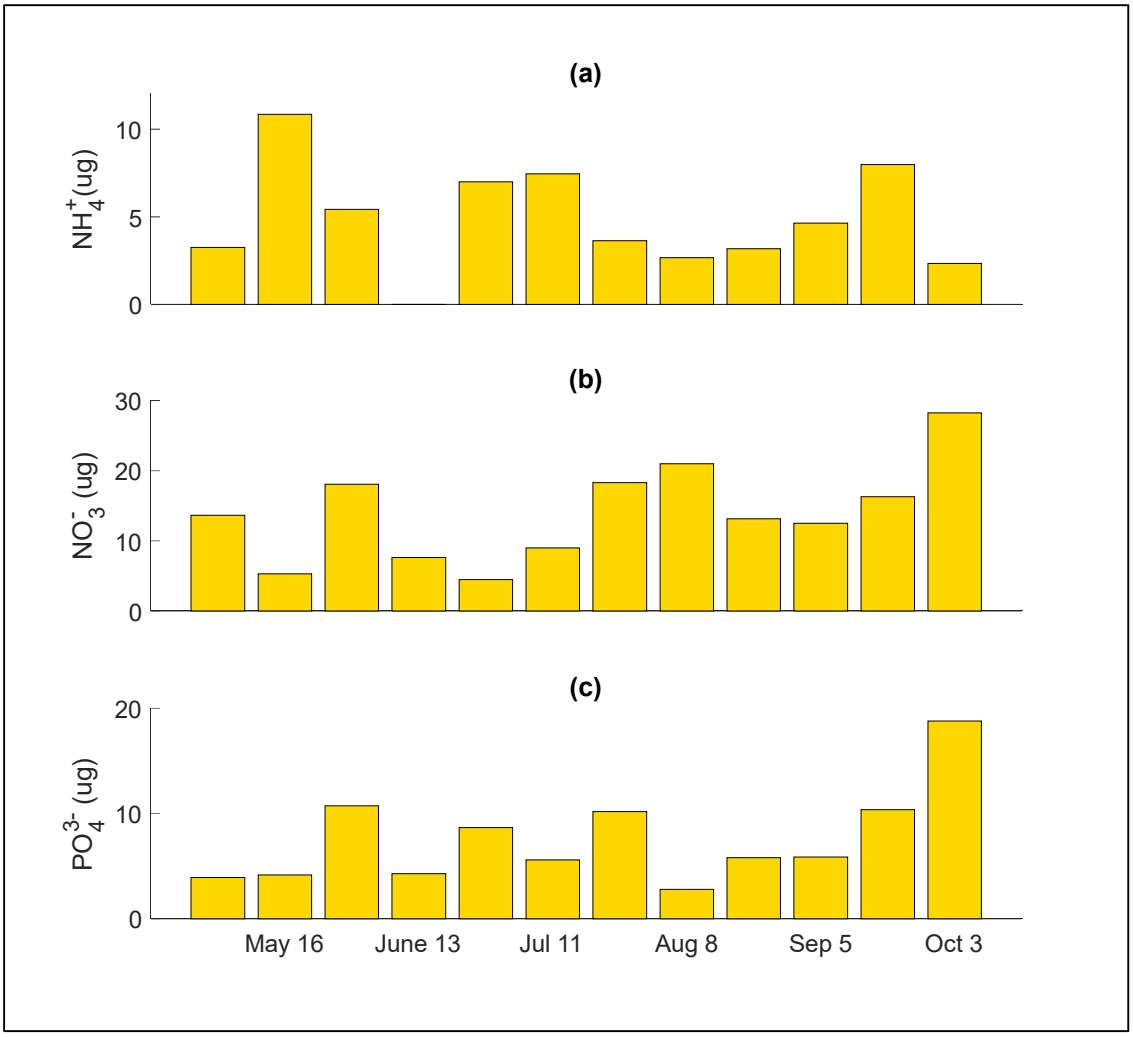

Figure 14: Seasonality of nutrients at the Green Roof. Ammonium (a), nitrate (b), and phosphate (c) are plotted as measured with IEM over the duration of the green roof study period, from April 18 to October 3. Ammonium was non-detect for the fourth observation interval, May 30 to June 13.

4.6.3 Regression Analysis

Altered model selection was required at the green roof. Multiple linear regression at the green roof was performed using a combination of backwards and forwards selection with the F-test. sample size of independent variables at the greenroof was low (n = 8), causing the creation of false “perfect” model fits with backwards selection. This was addressed by choosing models based on forwards selection to identify environmental

driver that were most likely to be explanatory variables with backwards selection. The backwards selection process was then conducted with the same methods used for the other sites but using a condensed list of explanatory variables rather than all possible variables.

Nutrient availability differed for each of the three nutrients, where precipitation was the most common driver, responsible at least in part, for availability of two nutrients. Ammonium availability was driven by a positive relationship with precipitation, and negative relationship with nitrate availability, together responsible for 73.8% of ammonium variability ($p = 0.01$). Nitrate availability was associated with a negative relationship with oxygen, an independent variable that was only present for part of the nutrient dataset length (Figure 15) . Oxygen never deviated from a concentration reading by more than a tenth of a percent, and oxygen was highly skewed at the green roof (coefficient of skewness = 1.06). Phosphate variability was positively associated precipitation, where 52.0% of variability was due to precipitation ($p = 0.00$,Table 4). Overall, ammonium availability was high when nitrate was low, and precipitation drove both ammonium and phosphate availability while nitrate was associated with the small observed changes in the skewed variable oxygen (Table 4).

Table 4: Statistical Parameters from multiple linear regression analysis in the Greenroof. Linear regression model coefficients, coefficient of determination (R^2) and p value significance tester are shown for each model.

Nutrient	Time	Precipitation	VWC	T_A	T_S	O_2	PO_4^{3-}	NH_4^+	NO_3^-	Adj. R^2	p
NH_4^+	-	0.4862	-	-	-	-	-	-	-0.7998	0.7382	0.0151
NO_3^-	-	-	-	-	-	-0.9137	-	-	-	0.6946	0.0062
PO_4^{3-}	-	0.7510	-	-	-	-	-	-	-	0.5210	0.0048

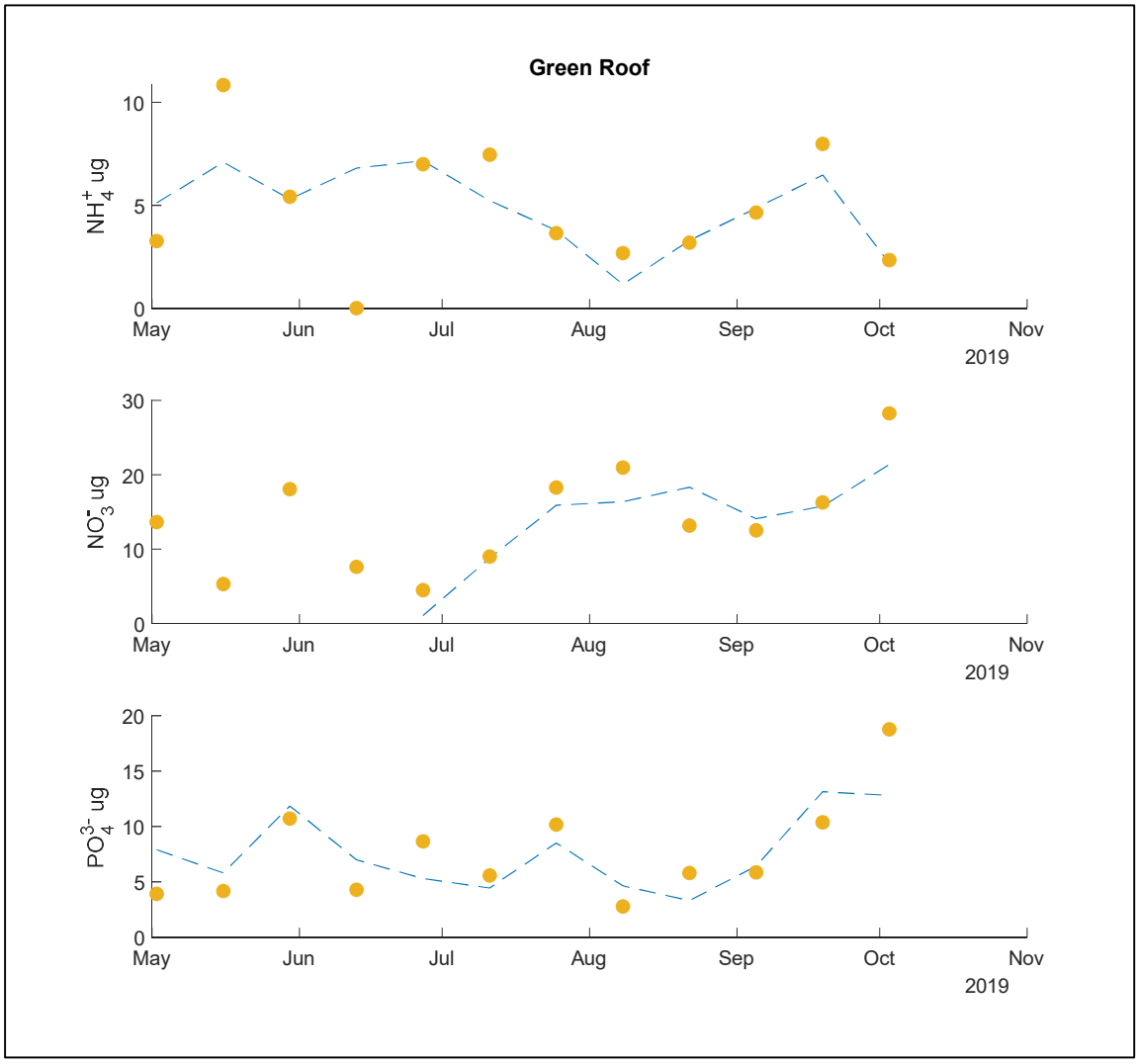

Figure 15: Multiple linear regression model results plotted against observed nutrient availability at the green roof. Plots of model output and observed data for ammonium, nitrate, and phosphate.

4.7 Constructed Stormwater Wetland

4.7.1 Environmental Drivers

Maximum daily precipitation occurred on July 20, with 2.0 inches of precipitation. The wettest observation interval was September 25 to October 9, with 4.3 inches of cumulative precipitation, and the driest cumulative interval was 0.03 inches from July 3 to July 17.

Soil moisture was significantly lower in the upland than in the lowland. Daily average soil moisture was 30.78 ± 9.07% in the upland, and 42.60% ± 1.67% in the lowland ($p = 0$). In the upland plot, soil moisture was dynamic and responsive to precipitation events (Figure 16b). Conversely, soil moisture in the lowland was less responsive to precipitation events and remained near saturation for the duration of the study. Lowland soil moisture did decrease slightly during extended inter-storm periods in the late summer (Figure 16b). The lowland plot was occasionally inundated with standing water from an adjacent permanent pool area during a few short periods following high precipitation events. Manual investigation at the lowland plot indicated the water table was at least 30 cm below the sensor depth.

Soil oxygen was significantly higher in the upland than in the lowland ($p = 0$). Soil oxygen was consistently near atmospheric oxygen concentration (20.95%) in the upland plot. Average soil oxygen was 18.28% ± 1.87% in the upland, and 10.33% ± 5.64% in the lowland. The lowest two-week soil oxygen content in the upland was the last observation, September 25 to October 9, but otherwise remained near atmospheric with a slight decrease in fall (Figure 16c). Lowland soil oxygen was more dynamic than the upland, peaking in late spring. The lowland had three intervals

with anoxic conditions (two-week average O_2 < 5%), July 3 -17, and back-to-back intervals September 11 – October 9 (Figure 16c).

Soil temperature followed similar seasonal patterns in the upland and lowland plots. Upland soil temperatures showed a larger diurnal range than lowland soil temperatures (Figure 16d). This was likely due to the high soil moisture and larger thermal capacity in the lowland soil.

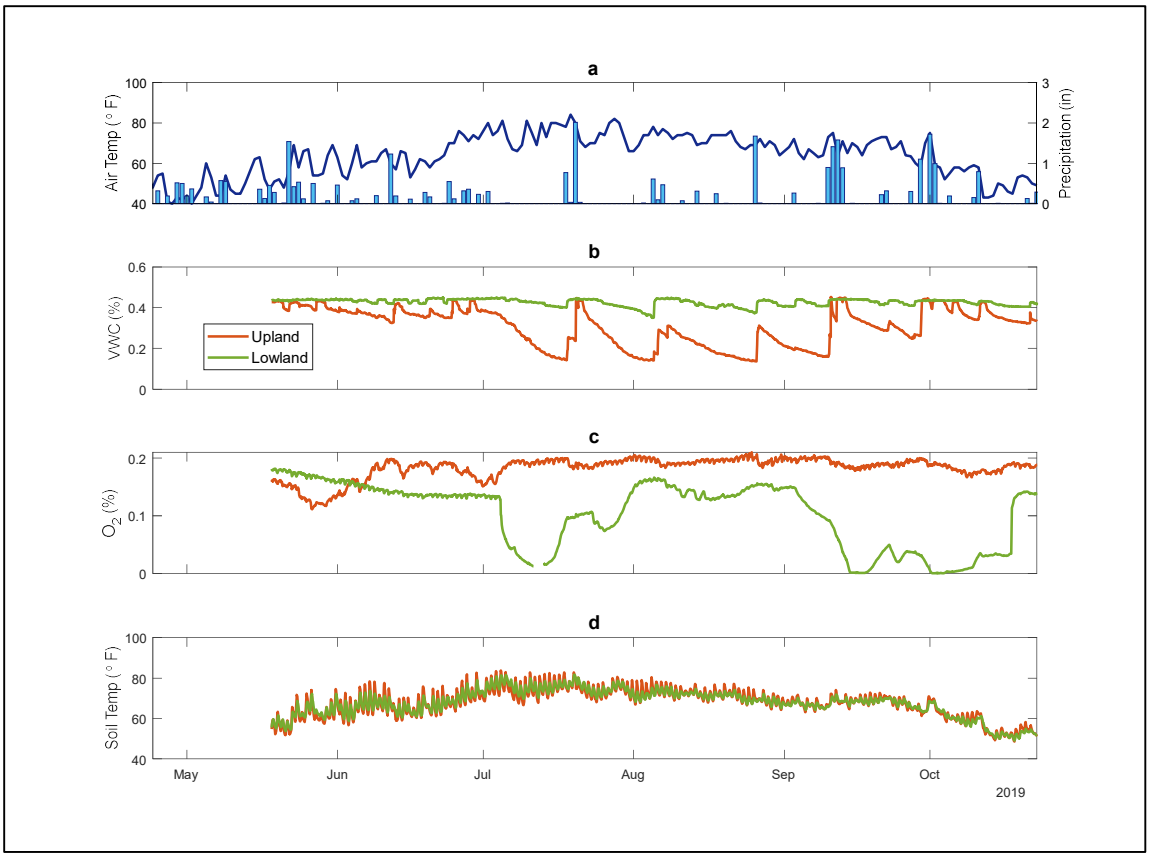

Figure 16: Seasonal variability in environmental drivers at the constructed stormwater wetland. Precipitation (a), air temperature (a), soil moisture (b), soil oxygen (c), and soil temperature (d). In-situ soil data was recorded at both an upland plot (orange) and a lowland plot (green). In-situ soil data are plotted at a 5-minute frequency, temperature is plotted as a daily average, and precipitation is plotted as a daily total.

4.7.2 Seasonality of Nutrient Availability

Averaged over the full study period, nitrate at the lowland was the most abundant of any nutrient (14.12 µg ± 15.69) at both locations. Nitrate was the second most available in the upland, with an average availability of 7.69 µg (±7.16). In both upland and lowland locations, nitrate availability had a wide range of availability across the 12 collection intervals (lowland: 2.20 µg - 55.16 µg; upland: 1.64 µg - 24.20 µg). Upland nitrate had high pulses in early spring, then remained relatively low until late summer (Figure 17). One upland nitrate observation was below the detection limit (June 19- July 3). Nitrate was generally more available in the lowland than upland, with higher availability in the lowland for 9 of 12 observations, two of which being the early-spring high upland pulses. Lowland nitrate was most available from mid-July to mid-August, with lower availability in the shoulder seasons (Figure 17).

Ammonium was the second most abundant nutrient at the lowland plot (3.17 µg ± 2.00) and the least abundant nutrient in the upland (3.37 µg ± 2.86). There was no significant difference between lowland and upland ammonium ($p = 1.35$ E-5). Upland ammonium was below the analytical detection limit for 4 of 12 intervals (May 22-June 5, July 31-August 14, August 14-August 28, September 25-October 9). Lowland ammonium was also below the detection limit for 4 intervals (April 24-May 8, June 5-June 19, September 11-September 25, September 25-October 9).

Phosphate was the least available nutrient in the lowland (2.91 µg ± 1.94), and most available in the upland (9.02 µg ±3.30). Upland PO_4^{3-} was higher than lowland PO_4^{3-} for every collection interval except July 3- July 17. Lowland PO_4^{3-} was generally lower in the shoulder months than in summer (Figure 17). Upland PO_4^{3-} had no

clear seasonal trend, but experienced high PO_4^{3-} pulses in late summer and moderate fall pulses.

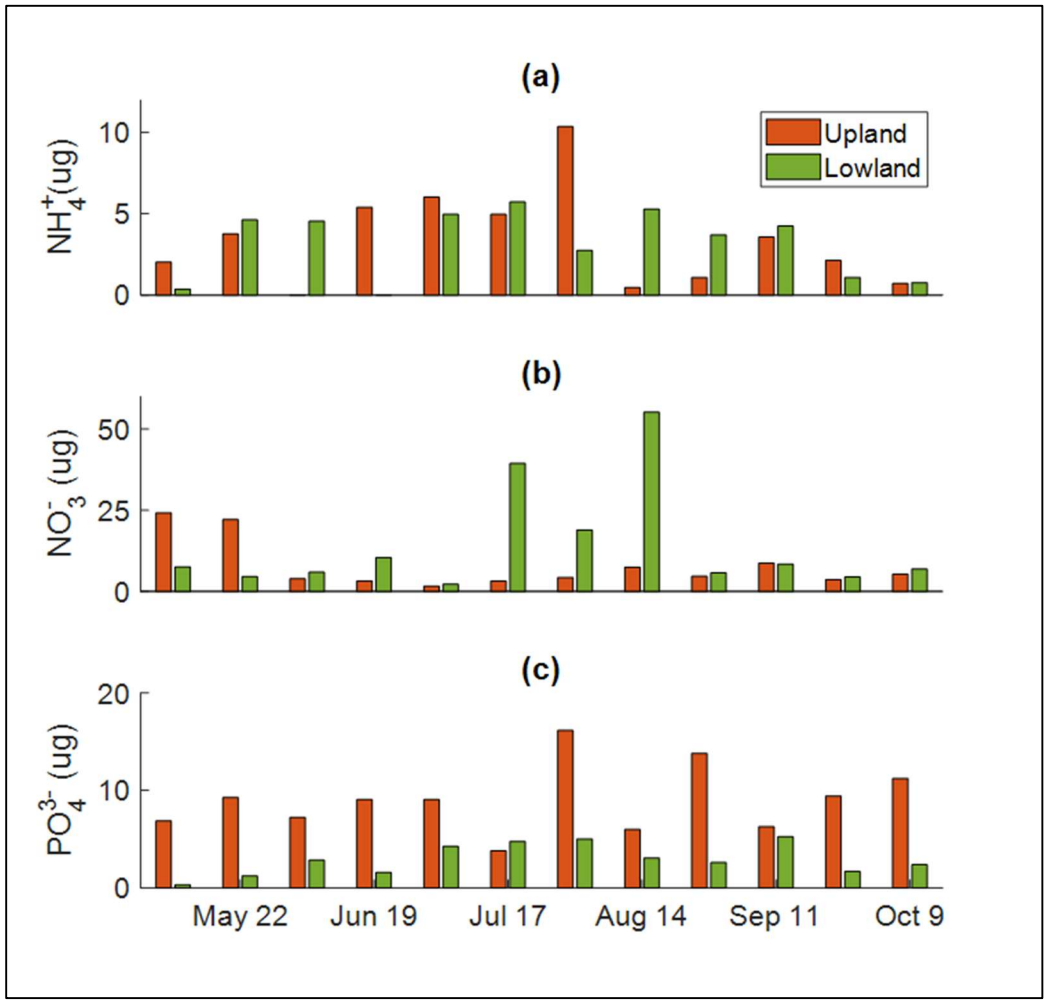

Figure 17 : Seasonality of nutrients at the constructed stormwater wetland. Ammonium (a), nitrate (b), and phosphate (c) are plotted as measured with IEM over the duration of the green roof study period, from April 24 to October 9. Wetland upland observations (orange) are plotted against wetland lowland observations (green). Ammonium was non-detect for the third interval at the upland (May 22 - June 5) and in the lowland fourth observation interval (June 5 - June 19).

4.7.3 Regression Analysis

Models were identified for 5 of the 6 nutrients in the upland and lowland, which explained 24% to 79% of the variability in nutrient availability. Only variability in upland ammonium could not be explained with a model. Amongst identified models, variation in nutrient availability was most often explained by precipitation and temperature. Precipitation was the most common explanatory variable, contributing to three of the identified models. Air temperature was identified in two models. Volumetric water content, soil oxygen, and time were explanatory in one model each. Neither soil temperature nor any of the nutrients contributed to the variability of any of the other nutrients at the wetland.

In the upland plot nitrate was negatively related to air temperature, and this variable alone explained 59% of nitrate availability in the upland ($p = 0.00$,Table 5) Phosphate in the upland was best explained by VWC, O_2, precipitation, and time. Interestingly, upland phosphate had a negative relationship with soil moisture, and positive relationship with precipitation.

In the lowland, both species were explained by negative relationships with precipitation. Only precipitation was valuable in explaining N species variability, contributing to 24% ($p = 0.06$) and 33% ($p = 0.03$) of the variability in ammonium and nitrate, respectively (Table 5). Lowland phosphate was also best explained by a single variable, air temperature, which contributed to 54% of the variability in phosphate ($p = 0.00$, Table 4). Lowland phosphate was generally more available during warmer periods, and both ammonium and nitrate were most available during dry periods.

In summary, while precipitation and air temperature had the strongest influence on nutrient availability in the constructed wetland, strength and direction of these relationships were dependent on landscape position (upland or lowland) and nutrient species. In the upland, precipitation was associated with increased phosphate and had no effect on ammonium or nitrate. While in the lowland, precipitation was associated with decreased N species and had no effect on phosphate. Further, temperature indicated a negative seasonal trend for upland nitrate, but was insignificant for lowland nitrate. Conversely, seasonality of upland phosphate was shown through a negative relationship with time, showing a decrease in phosphate over the full season, but in the lowland temperature indicated higher availability of phosphate in warm intervals. Availability of nutrients never had explanatory impact on other nutrients. Of all nutrients, ammonium was least well explained, defined only by a negative relationship with precipitation in the lowland (Figure 18).

Table 5: Statistical Parameter from multiple linear regression analysis in the constructed stormwater wetland. Linear regression model coefficients, coefficient of determination (R^2) and p value significance tester are shown for each model.

Nutrient	Time	Precipitation	VWC	T_A	T_S	O_2	Adj. R^2	p
Upland								
NH_4^+	-	-	-	-	-	-	-	-
NO_3^-	-	-	-	-0.7910	-	-	0.5887	0.0021
PO_4^{3-}	-1.9665	1.8361	-0.8150	-	-	1.2583	0.7887	0.0151
Lowland								
NH_4^+	-	-0.0500	-	-	-	-	0.2383	0.06128
NO_3^-	-	-0.6230	-	-	-	-	0.3273	0.0304
PO_4^{3-}	-	-	-	0.7610	-	-	0.5375	0.00403

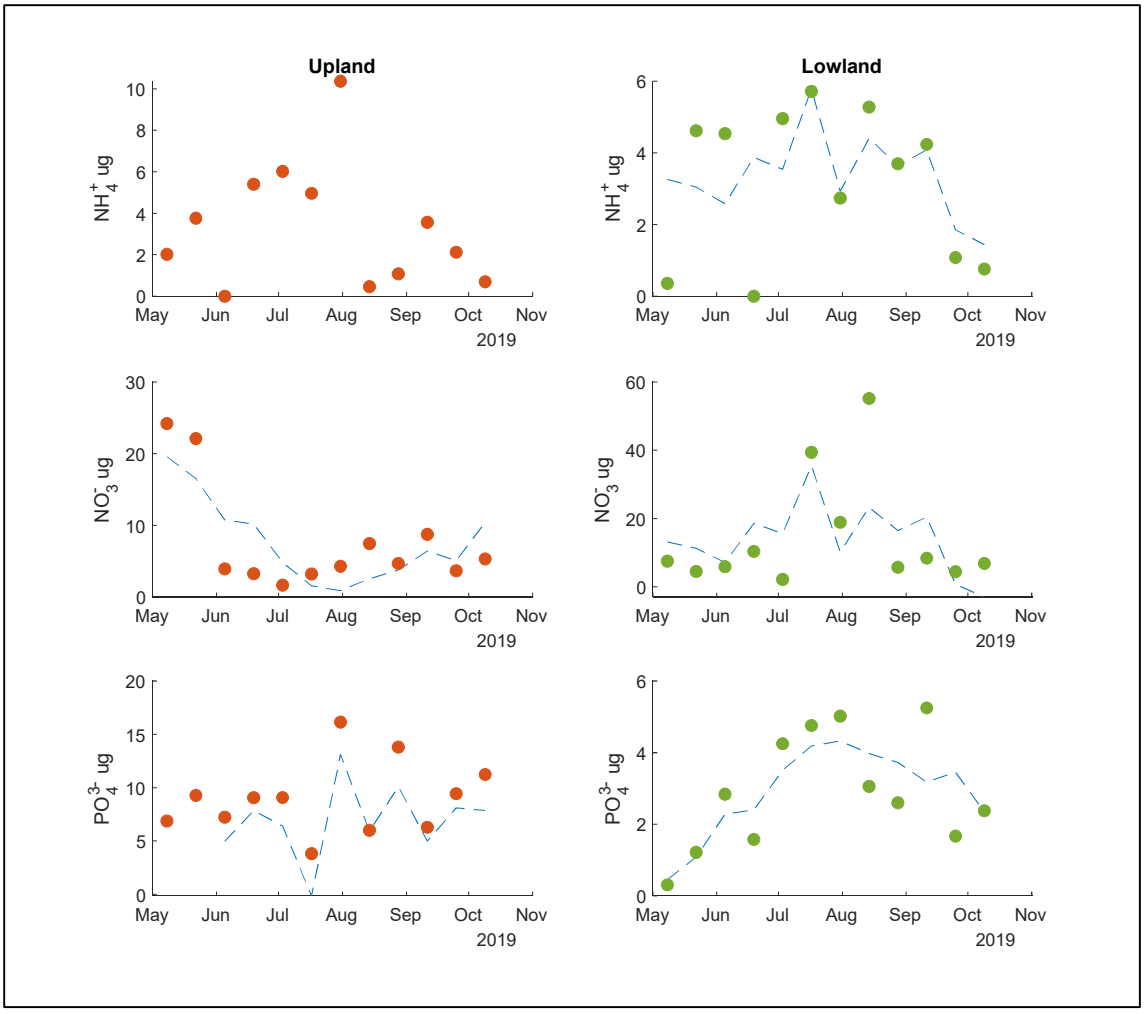

Figure 18: Multiple linear regression model results plotted against observed nutrient availability at the constructed wetland.

4.8 Site Comparison

When comparing the magnitude of nutrient availability at the three sites, ammonium was similar at all sites, but a greater mass of nitrate and phosphate was available at the garden plots than the other sites (Figure 19). Cumulative ammonium availability ranged from 38µg at the wetland lowland to 63.76µg at the East garden per $10cm^2$ for 24 weeks (Table 6), and average weekly observations ranged from 3.17µg at the wetland lowland to 5.31µg at the East Garden (Table 7). Nitrate availability varied

between sites, where nitrate availability at the gardens was >15 times higher than at the other sites. Nitrate availability ranged from 92.32 µg to 3647.2 µg cumulatively (Table 6), and 7.69 µg to 303.93 µg average weekly (Table 7), where in both cases nitrate availability was lowest at the wetland upland and highest at the East garden. Phosphate availability also varied between sites to a lesser degree as nitrate availability. Cumulative phosphate ranged from 34.94 µg to 437.19 µg (Table 6) and average availability ranged from 2.91 µg to 36.43 µg (Table 7), where availability was lowest at the wetland lowland and highest at the East garden. Nitrate was at least 15 times higher at the gardens than other sites and phosphate was at least 3 times greater at the gardens than other sites. The wetland lowland was the site with the lowest cumulative ammonium, average weekly ammonium, cumulative phosphate, and average weekly phosphate. The wetland lowland had the lowest cumulative nitrate availability and average weekly nitrate availability. The East garden had the highest availability of all nutrients measured both cumulatively and on an average weekly basis.

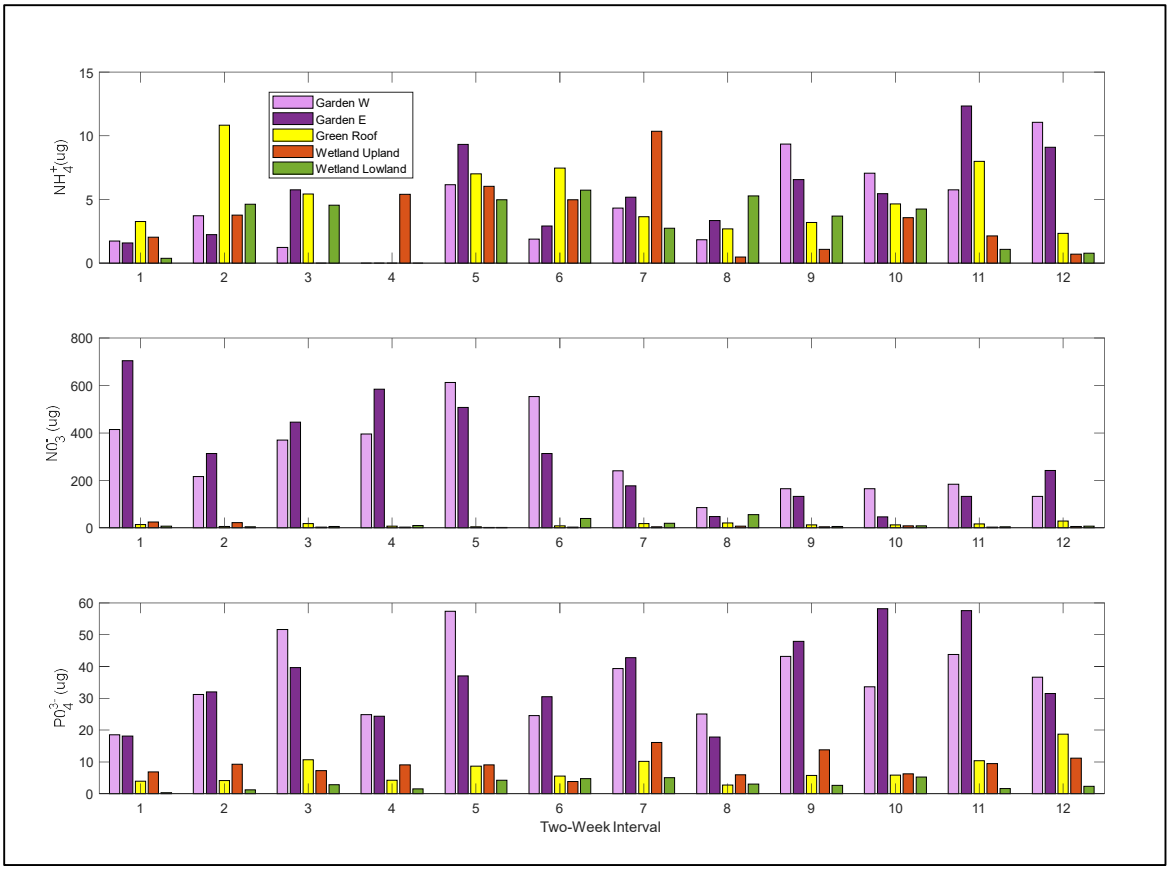

Figure 19: Comparison of availability of ammonium, nitrate, and phosphate at each of the 5 sites: the West and East urban garden plots, green roof, and constructed wetland upland and lowland.

Table 6: Comparison of cumulative mass of available nutrients observed at all study sites. Cumulative measurements account for the total mass of nutrient to accumulate on IEM of a 10cm^2 area over 24 weeks of observation, as determined by summing 12 2-week observations.

Nutrient	West Garden	East Garden	Green Roof	Upland	Lowland
NH_4^+	54.06	63.76	58.44	40.44	38.00
NO_3^-	3533.70	3647.20	167.62	92.32	169.46
PO_4^{3-}	429.66	437.19	91.07	108.20	34.94

Table 7: Comparison of average two-week available mass of nutrients observed at all study sites. Average measurements reflect the average availability of a nutrients, with units in $\mu g/10cm^2$/2-weeks.

Nutrient	West Garden	East Garden	Green Roof	Upland	Lowland
NH_4^+	4.51	5.31	4.87	3.37	3.17
NO_3^-	294.48	303.93	13.97	7.69	14.12
PO_4^{3-}	35.81	36.43	7.59	9.02	2.91

Identified models for nutrient availability varied between sites and nutrient type. Ammonium was associated with a positive relationship with time at both garden beds, and positive relationship with precipitation at the East garden and green roof, but a negative relationship with precipitation at the wetland lowland. Nitrate was negatively associated with time at the West garden, positively associated with air temperature the East Garden, negatively associated with O_2 at the green roof, negatively associated with T_a at the upland, and negatively associated with precipitation at the lowland. Phosphate had the most universal relationships, where phosphate availability was associated with increased precipitation at four of five sites, excluding the lowland. Phosphate was associated with only T_a at the wetland lowland. Phosphate was also negatively associated with time at the wetland upland, negatively associated with VWC at the East garden and upland, and positively associated with O_2 at the West garden and upland.

5. DISCUSSION

5.1 Ion Exchange Resins for GSI Monitoring

Studying nutrient availability with IERs allowed for novel observations of in-situ controls on nutrients. Monitoring site-specific nutrients has traditionally been done at GSI practices with measurements of nutrient concentrations of influent and effluent. These influent and effluent based monitoring techniques require adequate sampling volume, and sampling during or shortly following rainfall events. IERs allow for direct measurements of nutrient availability in soil. Advantages of nutrient observation with this method are freedom from rainfall-driven observation intervals, and ability to select observation intervals, and allowing for monitoring of urban green spaces without inlet and outlet structures for stormwater conveyance.

The use of IER bags in this study was unsuccessful due to incomplete desorption of collected nutrients in the ion extraction process. Lack of 100% desorption was identified as the source of error because during the first analysis of blanks (when the IER bags had not yet been buried in soil) blank values after extraction yielded observations of nearly 0. This indicated that the extraction and analysis process was not likely responsible for high blank values. Rather, as blanks were selected from IER bags which had been recycled from previous use in soil, these blanks returned non-zero values. Therefore, accumulation of ions must have been occurring on the IER despite the extraction process, and complete desorption of field ions must not have been occurring consistently. This led to unreliable readings of observations as it is unknown what percent of absorbed ions

were successfully extracted, and any collections made after incomplete desorption were unreliable, as the starting mass of ions on the IER bags was non-zero.

Two modes of error were identified for nutrient availability measurements conducted with IER bags. First, while incomplete extraction is known to exist, the percent of extraction achieved is unknown, and it is unknown whether the percentage of extracted ions achieved is variable with variable ion loading. For example, it is possible that 90% of nitrate is removed when measured nitrate was below 500 μg, but the same extraction methods only removed 60% of nitrate when detection was higher than 500 μg. Second, the ions remaining after extraction were carried over into the next field use of an IER bag so that in-situ accumulation onto the IER bag did not begin at zero. For these reasons, the IER bag data was unsuitable for use toward project goals. The IEMs were not recycled, and therefore did not have any accumulation.

However, with laboratory experimentation, the recycled use of IERs for in-situ nutrient observation is viable. To successfully employ IER bags in the field, an appropriate extractant concentration and extraction time would need to be identified for the range of adsorbed ions expected. This could be accomplished by deploying multiple IER bags in the field for the expected observation interval desired for the experiment, then extracting these IER bags at a range of concentrations and extractions lengths, beginning at 1 M eluent concentration with a 1 hour extraction, as used in the methods of this project. Then extracted bags would go through a second extraction process to determine if there was any ion carry-over from the first extraction. This would be repeated until extractant concentrations were measured at zero. Conducting this test to identify extraction concentration and time would be necessary for all ranges of nutrients

expected to be collected in the study. It is recommended that in all future uses of IER bags a similar required-extraction procedure is followed to ensure that complete extraction is performed for all observation intervals, and the continued use of blanks would be necessary as a check of complete extraction over the course of the study period.

5.2 Soil Oxygen Dynamics

Soil oxygen content is indicative of the presence of different biogeochemical processes in a soil system and can be used to understand the ecohydrological processing of nutrients. The most prominent example of O_2 controls on N and P processing is through N cycling. With necessary carbon stock for the microbial population, aerobic soil conditions promote nitrate production through nitrification and anoxic conditions stimulate the reduction of nitrate to N-gas through denitrification. Therefore, by understanding the oxygen status of the soil, assumptions can be made about whether nitrate is being produced or consumed by the soil microbes. Therefore, understanding soil oxygen dynamics in urban green spaces is key to understanding the processing of nutrients in soils.

Soil oxygen was generally high and stable at the urban garden plots and green roof, but wetland oxygen was more dynamic, especially at the lowland plot. While diurnal soil oxygen was apparent, very little fluctuation in O_2 occurred seasonally at the garden plots. Both the West and East plot showed decreased soil oxygen during sudden heavy precipitation, like the events in mid-July and mid-September (Figure 16). The green roof was even less dynamic, as no notable changes in soil oxygen were observed during precipitation events. While the garden plots and green roof do not receive stormwater larger than their surface area (receive no drainage or overland flow), the

difference in O_2 response to precipitation events is likely due to the varying soil media and design. The urban gardens consist of deeper loamy organic soil with no outlet or drainage, while the green roof is coarse and porous with an underdrain. Therefore, ponding and pore space saturation to the point of soil oxygen displacement is logical for the urban gardens, and consistently high oxygen is consistent with green roof expectations.

Upland O_2 displayed reactions to precipitation similar to those observed at the urban gardens, but the lowland O_2 was highly dynamic and widely ranging, suggesting that lowland soil oxygen fluctuations are associated with more than precipitation (Figure 16). Lowland O_2 decreased gradually from mid-May to early July when precipitation was frequent, then decreased rapidly in the first week of July during a long dry period, and finally increased again through the end of July. A second anoxic period occurred in September and October. In contrast to the first, the second period was associated with relatively wet and cool conditions.

The observed seasonality of lowland O_2 can be explained by (1) the direct effects of seasonal change in temperature and precipitation on physical soil changes, and (2) the effect of seasonal temperature and precipitation on microbial oxygen consumption. During the prolonged period without precipitation in early July, oxygen quickly decreased to anoxic conditions. The combined dry conditions and decrease in oxygen indicate that oxygen was being consumed by microbes and plants, as the increase in temperatures would have increased microbial metabolism and plant growth to support leaf development. Additionally, the high VWC during this time likely assisted in creating low oxygen conditions by preventing reaeration from the soil surface with atmospheric

oxygen. Shortly after reaching aerobic conditions, O_2 began to increase in the soil. This reaeration may be due to atmospheric oxygen seeping through macropores. Soil in the lowland was defined by fine texture and the soil surface was observed cracked during prolonged dry periods in the summer. The creating of these macropores (cracks) may have allowed deep infiltration of atmospheric oxygen into the soil to promote reoxygenation. During this July reoxygenation, a heavy precipitation event occurred, slowing reoxygenation for a time (likely until standing water receded), at which point reoxygenation continued. This occurrence fits with the logic of macropore reaeration, as the precipitation would have inundated the lowland, creating temporary clogging of pores and low O_2.

In contrast, the second anaerobic period was caused by an onset of several heavy precipitation events. In July, precipitation slowed the reoxygenation rate, but in September, heavy precipitation expedited deoxygenation to the point of anoxia. Again, once oxygen depleted, reoxygenation began, and again, precipitation during reoxygenation slowed the rate of reoxygenation. This fall precipitation during the second post-anoxic aeration returned soil to anoxic conditions. The October rebound of O_2 following fall anoxic conditions was likely due to a decrease in oxygen consumption. Fall temperatures would have suppressed aerobic microbial metabolism and photosynthesis, resulting in higher O_2. The rapid reoxygenation of lowland soil in October closely paralleled rapid fall oxygenation unprompted by precipitation in a natural wetland in Millbrook NY. In this case, rapid fall reoxygenation was attributed to the drying of macropores so that atmospheric oxygen was able to enter soils, in combination with plant senescence (Burgin & Groffman, 2012).

The relationship between O_2 and VWC varied between the different sites, indicating that the common perception of a negative relationship between VWC and O_2 is an oversimplification. VWC is commonly used to estimate O_2 because of conceptual understanding that increased VWC means increased occupation of water in soil pore space, thus driving out soil oxygen. This O_2 estimation has been performed with linear estimations and nonlinear estimations (Calabrese & Porporato, 2019; Hall, McDowell, & Silver, 2013). The compiled VWC and O_2 data for all sites used in this study closely resemble the relationship observed by Hall et al. (2013). However, the soil oxygen dynamics at the wetland lowland indicates that antecedent moisture conditions, seasonal context, and hydrologic residence time, also play a role in determining the quantity of O_2. Therefore, estimation of O_2 with solely VWC may portray an incomplete and oversimplistic story of O_2 in soil. In GSI, it is important to understand soil O_2 in the context of microbial activity, which affects biochemical processing of nutrients and GHG production, like methane and nitrous oxide (Bledsoe et al., 2020; Ebrahimi & Or, 2016; Jarecke, Loecke, & Burgin, 2016). Accounting for antecedent conditions, seasonal context and hydrologic residence time in soil oxygen estimations can improve estimations of GHG release.

5.3 N seasonality and the creation of ideal nitrification conditions

The availability of N-species was influenced by biogeochemical variability influencing nitrification to create summertime periods with high nitrate availability, with different driving factors depending on soil characteristics. Previous studies of nitrate or nitrification seasonality have shown contrasting results. A stormwater trench observed low summertime available nitrate, attributing this drop to anoxic conditions created in the

summer (Mullins et al., 2020). A constructed stormwater wetland also observed higher denitrification potential in spring and summer than fall and winter (Bledsoe et al., 2020). However, both a greenroof and natural riparian zone experienced summertime nitrate peaks, where the riparian zone suggest seasonally-induced nitrification as the mechanisms responsible for high nitrate (Buffam et al., 2016; Duncan et al., 2015). In this work, observations at the urban garden plots and constructed stormwater wetland agree with the general seasonal trend observed by Buffam et al. and Duncan et al. where nitrate was more available during certain summer intervals. Observations of N species availability at the wetland reveals that biogeochemical controls are dominant in N species in hydrologically dynamic green spaces.

The most notable changes in N availability at the lowland were high summertime nitrate pulses (July 3-August 14). Possible explanations for this increase in available nitrate are mechanisms associated with decreased removal or retention and increased inputs, e.g., decreased biological uptake, increased N in influent, and nitrification induced through aerobic conditions. Evidence for these explanations is evaluated using air and soil temperature as proxies of biological activity, soil oxygen dynamics to infer soil status as nitrifying or denitrifying, and precipitation as a vector of possible inputs.

Lowland nitrate peaked in late summer (July 3-August 14) during observation intervals with the three highest soil and air temperatures, with varying cumulative two-week precipitation volumes. During these warm-weather periods plant activity was high, leading to the conclusion that plant uptake (or lack thereof) was not responsible for summer nitrate pulses because high plant activity would cause lower available nitrate due to plant uptake. Additionally, high summertime anthropogenic inputs (i.e., fertilizers) are

unlikely to drive high summer availability, as this N source would be associated with increased precipitation, acting as a vector to bring nitrate into the wetland (assuming dry atmospheric deposition is a minor contributor at the scale of the wetland). However, the observed strong negative relationship between lowland nitrate and precipitation shows that exterior sources are likely not the cause of high summertime availability. Observations of precipitation and plant growth inferences indicate that high pulses of lowland nitrate availability in summer were not caused by seasonality of plant uptake or anthropogenic inputs.

The creation of nitrifying conditions due to the combination of biogeochemical factors best explains the occurrence of summertime peaks in lowland nitrate. The dependency of nitrate availability on nitrification is most evident in the high explanatory power of precipitation on nitrate availability in the lowland. The negative relationship between lowland nitrate availability and precipitation indicates that during observation intervals with low cumulative precipitation nitrate was most available. This fits into the logical chain of biogeochemical triggers creating nitrifying conditions: lack of precipitation causing decreased soil moisture, and increased oxygen in soil pore space, therefore creating aerobic conditions. Warm temperatures, combined with an 11-day period without precipitation dried lowland soils to the point of cracking, creating macropores that would promote higher soil oxygen. Cumulative antecedent dry conditions, macropore cracking, and warm temperatures created ideal conditions for aerobic, warm temperature thriving nitrifiers, which then produced nitrate, creating a pool of available nitrate, which was then mobilized during the proceeding precipitation event and resulted in high available nitrate.

This nitrification-reliant explanation is further supported by other field observations of high summertime nitrate. In a natural riparian zone in Maryland, June-September peaks in stream nitrate were attributed to the seasonal aeration of riparian zones by temperature increase and groundwater dynamics to stimulate nitrification in formerly denitrifying zones (Duncan et al., 2015).

In the upland, nitrate was relatively stable over the course of the season, and variability was modeled by a negative relationship with temperature. While the seasonality pattern observed in the upland agreed with nitrate seasonality observations by Mullins et al., 2020 and Bledsoe et al., 2020, both of these works attributed seasonal observations to the presence of summertime denitrification. However, there is no evidence in biogeochemical or hydroclimatic observations that denitrification was the major contributor of warm-weather low nitrate availability in the upland. The observation of higher nitrate availability in cooler observation intervals may be driven by the two highest upland nitrate observations occurring in the cool spring. Similar high nitrate pulses in April and early May are also seen at the garden plots. High cumulative precipitation in the spring and lack of microbial and plant activity may have produced these observations as it may have been too cold for microbial performance of denitrification, plant growth is low, and high precipitation would mobilize any pooled nitrate that may have accumulated during winter months when biological uptake would have been low from low microbial metabolism and plant senescence.

While different explanatory variables were identified for N species in the East and West garden plots, both plots reflect the seasonal dynamics observed in the wetland upland. In both garden plots and the upland, nitrate had an observable trend in

seasonality, where nitrate generally peaked in late June, then decreased until August, after which point availability remained consistent.

This contrast between a temperature driven nitrate regime in the upland, against the ideal biogeochemical nitrification conditions that dominated lowland nitrate availability highlight the sensitivity of the constructed wetland to environmental drivers. Lowland areas of wetlands and trenches (also called wet zones) have been shown in multiple studies to be dominated by denitrification due to their saturated, anerobic soil conditions, and thus are capable of decreasing available nitrate (Bledsoe et al., 2020; L. E. McPhillips et al., 2016; L. McPhillips et al., 2018; Morse et al., 2017; Mullins et al., 2020). However, this work shows that in summer time under dry conditions, it is possible that lowland zones of constructed wetlands may transition to aerobic conditions under which nitrification becomes the predominant stage of N cycling and nitrate pools are developed in soil. This observation aligns with a field study of a predominant denitrifying riparian zone converting to nitrification during warm summer conditions (Duncan et al., 2015).

In sites where O_2 was high, N species displayed higher availability in spring and summer than fall, but where VWC was high and O_2 was dynamic, peaks and lows in nitrate availability aligned logically with the conditions expected for nitrification and denitrification, suggesting that these processes may play a larger role in lowland nitrate availability. Green roof N species were least well explained, where the most notable trend in availability was increased ammonium availability during times of high cumulative precipitation. The West and East garden plots indicated that nitrate was more available earlier in the study period, and during times of warmer temperatures,

respectively, both seeming to represent a late-June, early-July peak in nitrate through different explanatory variables. The wetland was the most dynamic of the three sites, showing a sharp contrast where the upland displayed similar seasonal variation as observed at the urban gardens, but lowland nitrate availability was strongly controlled by biogeochemically induced N cycling, resulting in summertime spikes in nitrate availability from ideal conditions for nitrification.

5.4 Phosphate Availability Driven by Physical Mobilization

Phosphate availability was driven by increased transport from precipitation. In the four sites with highly varying soil moisture, East and West garden plots, the green roof, and the wetland upland, precipitation was selected as a contributing variable in models of phosphate availability. Other explanatory variables included a negative association with VWC (East garden plot, wetland upland), as well as time and oxygen at the upland (both positively related to phosphate availability). The only site in which phosphate variability was not related to precipitation was the wetland lowland. This stark contrast between the wetland lowland and all other sites suggest that the physical transport of phosphate by precipitation mobilizes phosphate in soils, as shown in the garden plots, green roof, and wetland upland. This increased mobilization may not occur in sites with high soil moisture, like the wetland lowland.

Despite ecological importance in limiting eutrophication, P retention in GSI is variable, even yielding negative removal rates (Adyel, Hipsey, & Oldham, 2017; Duan, Newcomer-Johnson, Mayer, & Kaushal, 2016; Frost, Prater, Scott, Song, & Xenopoulos, 2019; J. Li & Davis, 2016). High variability in P retention may be due to the impact of seasonality on inflowing P, the uptake of P, or speciation of P. For example, seasonal

draining alters P species to more bioavailable forms (Olila, Reddy, & Stites, 1997). In this study, observations of contrasting phosphate availability between sites with varying VWC and the lowland plot offer insight as to what conditions result in easily mobilized phosphate.

The observed positive relationships between phosphate availability and precipitation at the upland, West and East plot of the urban gardens, and at the green roof may be due to three possible mechanisms: wet atmospheric deposition, loading from stormwater inflow, and mobilization of pooled soil phosphate. The first two possible causes of increased availability consider the increased phosphate to be increases due to inflows brought into the soil system by precipitation (directly in precipitation for atmospheric deposition, and through stormwater conveyance for stormwater loading). Precipitation has been shown to contribute P in this manner in previous studies where wet and dry atmospheric deposition can be a significant source of P, estimated as 13-33% of total P watershed inputs in Minneapolis, MN (Hobbie et al., 2017), and phosphate is commonly observed in stormwater influent samples.

However, it is unlikely that phosphate availability was increased from inflowing phosphate with precipitation in this study. If precipitation did increase P loading, then the lowland site would be expected to have at least the same increase in phosphate availability with precipitation, if not greater due to its larger drainage are to surface area ratio. Thus, it is most likely that the root cause of the phosphate and precipitation relationship is the promotion of phosphate mobility because of increased precipitation. Since measures of IEM availability are contingent upon mobility and phosphate is a dissolved phosphorus form, it is likely that increased precipitation was able to mobilize

phosphate already present in the soil. This indicates that phosphate mobility in the upland, urban gardens and green roof was more heavily controlled by soil phosphate pools than inflowing phosphate, which aligns with previous studies emphasizing the importance of organic matter decomposition in P dynamics in urban ecosystems (Frost et al., 2019; Selbig, 2016; Song, Winters, Xenopoulos, Marsalek, & Frost, 2017; Song, Xenopoulos, Marsalek, & Frost, 2015). High pulses of phosphate availability at the upland in fall further align with this concept of organic P matter decomposition playing a key role because in fall plant senescence is expected, and precipitation was high, serving as a means to increase the phosphate pool, and to mobilize that labile phosphate, creating the observed high fall phosphate availability

Where precipitation served as a means of phosphate availability in the other study sites, lowland phosphate was not strongly related to precipitation, but rather to air temperature. Contrary to expectations, phosphate availability was consistently lower at the lowland than at the upland. Roughly half of lowland phosphate variability was associated with air temperature, indicating a strong seasonal dependency. This seasonality is contrary to expectations based on wetland plant activity, which were expected to have highest nutrient uptake in summer causing reduced available phosphate (Trentman et al., 2020). This anticipated heightened summer uptake may be lower at the lowland than other sites, or warm-weather inputs may have overpowered increased summer biological uptake. Without measurements of site-specific input and uptake mechanisms, the direct source of summertime phosphate peaks in the lowland cannot be distinguished.

At sites with variable soil moisture, phosphate availability is driven by the increased mobility provided by precipitation in soils where precipitation influences soil moisture. The identification of physical mobilization of soil phosphate as the major contributor of phosphate availability is promising, as phosphate can be limited by performing organic matter removal like rowing, and leaf litter pick-up (Erickson et al., 2018). Through the removal of organic matter from the surface of urban soils in routine maintenance, the source of phosphate pools would be diminished, decreasing the ability for precipitation to mobilize this pooled soil phosphate.

6. CONCLUSIONS

6.1 Key Findings

This work has contributed to further the understanding of urban nutrient cycling. Meaningful contributions include the observation of seasonal nutrient availability in urban green spaces, indication that lowland zones may be converted to predominantly nitrifying zones during dry summer conditions, and the identification of increasing phosphate availability with increasing precipitation depending on dominant soil moisture regime.

This work reports novel observations of in-situ nutrient availability in urban areas over the course of a growing season. These observations were monitored with tools commonly employed in other geoscience fields, but not yet applied to environmental engineering for the purpose of urban nutrient management. Knowledge of the seasonal availability helps to identify environmental scenarios when nutrient leaching from urban soils is most likely. Further, the environmental drivers identified to contribute to nutrient variability offer insight to mechanisms applicable to urban soils beyond those studied here.

The observed threshold-defined relationship between VWC and soil oxygen content confirms the need for decoupling these two variables in urban ecosystem modeling. Similar observations of the VWC and oxygen content relationship have been shown in previous studies, but its applicability to urban soils is confirmed in this work. Decoupling VWC and oxygen in ecosystem models can help to improve the accuracy of

these models, especially in the forecasting of aerobic and anaerobic conditions critical for identifying which nutrient cycling processes are dominant.

Urban soils with high soil moisture are susceptible to exporting high nitrate concentrations during drying events in summertime. Observations of summertime pulses in nitrate availability at the constructed wetland lowland are similar to seasonal nitrate peaks in stream flow concentrations coming from the aeration of predominantly anoxic stream banks, both confirming nitrification as the likely cause, and suggesting a larger consequence of heightened summertime nitrate in waterbodies close to saturated urban soils.

Finally, two driving P availability mechanisms were identified: precipitation in aerated soils and air temperature in saturated soils. These identified drivers of urban phosphate availability suggest that mobilization of soil P pools is the greatest contributor to phosphate availability. This is particularly impactful as P plays a critical role in freshwater eutrophication, thus urban green space design can be improved to mitigate the anticipated mobilization of labile soil phosphate following precipitation events.

6.2 Future Work

A potential limitation in IER use for green space nutrient monitoring is the disconnect between observations of high relative in-situ nutrient availability and water quality. Both a qualitative and quantitative gap exists. It is unknown whether the trends of higher and lower relative availability of nutrients in soil would parallel trends in effluent water quality from urban soils, and if the trends are parallel, whether the patterns observed in soil availability would be amplified or dampened in effluent water quality observations. This knowledge could be gained by monitoring both in situ nutrient

availability and traditional influent and effluent at a GSI practice. The sampling process would involve the burial of IEMs from the conclusion of one storm to the next, mirroring the frequency of influent and effluent data collection. In doing this, any nutrient cycling occurring proceeding a storm event would be known, as the nutrients made available preceding a storm event would be mobilized and measured during the following storm event. By monitoring both in-situ soil nutrient availability with IERs and influent and effluent concentrations, the relationship between in situ soil nutrient availability and effluent water quality could be identified.

Use of IEMs in this work was successful in monitoring available nutrients, but methods in the future could be expanded to the application of IER bag use if desorption from IER bags is better quantified. In future work, complete desorption of collected ions from IER bags could be achieved by testing a variety of extraction concentrations and extraction times. Employing IER bags with successful extraction methods would allow for longer-term (multi-month) use of IERs for nutrient monitoring, an advantage of IER bags over IEMs.

Finally, to best understand and apply the contributions gained through this work, it is important to conduct multi-season observations of nutrient availability and environmental drivers at these and other urban green spaces. The observations made over this growing season could increase confidence with repeated seasonal observation in following years. Identifying relationships between seasonality and nutrient availability at other urban green spaces would also be valuable in expanding understanding of the possible variation in these relationships between different types of sites.

7. BIBLIOGRAPHY

Adyel, T. M., Hipsey, M. R., & Oldham, C. E. (2017). Temporal dynamics of stormwater nutrient attenuation of an urban constructed wetland experiencing summer low flows and macrophyte senescence. *Ecological Engineering*, *102*, 641–661. https://doi.org/10.1016/j.ecoleng.2016.12.026

Allenby, B. R. (2012). *The theory and practice of environmnetal engineering*. Upper Saddle River: Prentice Hall.

Amundson, R., Berhe, A. A., Hopmans, J. W., Olson, C., Sztein, A. E., & Sparks, D. L. (2015). Soil and human security in the 21st century. *Science*, *348*(6235). https://doi.org/10.1126/science.1261071

Anderson, D. M., Glibert, Patricia, M., & Burkholder, J. M. (2002). Harmful Algal Blooms and Eutrophication Nutrient Sources , Composition , and Consequences. *Estuaries*, *25*(4), 704–726.

Ator, S. W., Webber, J. S., & Chanat, J. G. (2020). Factors driving nutrient trends in streams of the Chesapeake Bay watershed. *Journal of Environmental Quality*, (May), 1–23. https://doi.org/10.1002/jeq2.20101

Bailey Boomer, K. M., & Bedford, B. L. (2008). Groundwater-induced redox-gradients control soil properties and phosphorus availability across four headwater wetlands , New York , USA. *Biogeochemistry*, *90*, 259–274. https://doi.org/10.1007/s10533-008-9251-2

Band, L. E., Tague, C. L., Groffman, P., & Belt, K. (2001). Forest ecosystem processes at the watershed scale : hydrological and ecological controls of nitrogen export. *Hydrological Processes*, *15*(July 2000), 2013–2028. https://doi.org/10.1002/hyp.253

Bennett, E. M., Carpenter, S. R., & Caraco, N. F. (2001). Human Impact on Erodable Phosphorus and Eutrophication : A Global Perspective. *BioScience*, *51*(3), 227–234.

Bergquist, L. (2018, July 30). Dead zones in Green Bay show signs of lasting longer, raising long-term questions. *Milwaukee Journal Sentinel*. Retrieved from https://www.jsonline.com/story/news/local/wisconsin/2018/07/30/green-bays-dead-zones-raise-long-term-questions-over-health-bay/844073002/

Billings, S. A., Schaeffer, S. M., & Evans, R. D. (2004). Soil microbial activity and N availability with elevated CO 2 in Mojave Desert soils. *Global Biogeochemical Cycles*, *18*, 1–11. https://doi.org/10.1029/2003GB002137

Bledsoe, R. B., Bean, E. Z., Austin, S. S., & Peralta, A. L. (2020). A microbial perspective on balancing trade-o ff s in ecosystem functions in a constructed

stormwater wetland. *Ecological Engineering*, *158*(August), 106000. https://doi.org/10.1016/j.ecoleng.2020.106000

Boardman, E., Efi, M. D., Dolph, C. L., & Finlay, J. C. (2019). Fertilizer , landscape features and climate regulate phosphorus retention and river export in diverse Midwestern watersheds. *Biogeochemistry*, *146*(3), 293–309. https://doi.org/10.1007/s10533-019-00623-z

Bremer, E., Miller, J. J., & Curtis, T. (2018). Placement of ion-exchange membranes for monitoring nutrient release from flooded soils, *715*(November), 709–715.

Brookshire, J., Gerber, S., Webster, J. R., Vose, J. M., & Swank, W. T. (2011). Direct effects of temperature on forest nitrogen cycling revealed through analysis of long-term watershed records. *Global Change Biology*, *17*, 297–308. https://doi.org/10.1111/j.1365-2486.2010.02245.x

Buffam, I., Mitchell, M. E., & Durtsche, R. D. (2016). Environmental drivers of seasonal variation in green roof runoff water quality. *Ecological Engineering*, *91*, 506–514. https://doi.org/10.1016/j.ecoleng.2016.02.044

Burgin, A. J., & Groffman, P. M. (2012). Soil O 2 controls denitrification rates and N 2 O yield in a riparian wetland. *Journal of Geophysical Research*, *117*(November 2011), 1–10. https://doi.org/10.1029/2011JG001799

Calabrese, S., & Porporato, A. (2019). Impact of ecohydrological fl uctuations on iron-redox cycling. *Soil Biology and Biochemistry*, *133*(February), 188–195. https://doi.org/10.1016/j.soilbio.2019.03.013

Carey, R. O., Hochmuth, G. J., Martinez, C. J., Boyer, T. H., Dukes, M. D., Toor, G. S., & Cisar, J. L. (2013). Evaluating nutrient impacts in urban watersheds : Challenges and research opportunities. *Environmental Pollution*, *173*, 138–149. https://doi.org/10.1016/j.envpol.2012.10.004

Carpenter, S. R. (2008). Phosphorus control is critical to mitigating eutrophication. *PNAS*, *105*(32), 11039–11040.

Center for Watershed Protection. (2007). *National Pollutant Removal Performance Database*. Ellicott City, MD.

Childers, D. L., Bois, P., Hartnett, H. E., Mcphearson, T., Geneviève, S., & Sanchez, C. A. (2019). Urban Ecological Infrastructure : An inclusive concept for the non-built urban environment. *Elementa Science of the Anhropocene*, *7*(46).

The Clean Water Act, 1977. 33 U.S.C. § 502.

Collin, A., Messier, C., & Belanger, N. (2017). Conifer Presence May Negatively Affect Sugar Maple ' s Ability to Migrate into the Boreal Forest Through Reduced Foliar Nutritional Status. *Ecosystems*, *20*, 701–716. https://doi.org/10.1007/s10021-016-

0045-4

Cooperband, L. R., Gale, P. M., & Comerford, N. B. (1999). Refinement of the Anion Exchange Membrane Method for Soluble Phosphorus Measurement. *Soil Sci. Soc. Am. J.*, *63*, 58–64.

Cooperband, L. R., & Logan, T. . J. (1994). Measuring In Situ Changes in Labile Soil Phosphorus with Anion-Exchange Membranes. *Soil Sci. Soc. Am. J.*, *58*, 105–114.

D'Odorico, P., & Rigon, R. (2003). Hillslope and channel contributions to the hydrologic response. *Water Resources Research*, *39*(5), 1–9. https://doi.org/10.1029/2002WR001708

Davis, A. P., Shokouhian, M., Sharma, H., & Minami, C. (2006). Water Quality Improvement through Bioretention Media : Nitrogen and Phosphorus Removal. *Water Envirornment Research*, *78*(3), 284–293.

Department of Environmental Conservation, . (2015). *New York State Stormwater Management Design Manual*.

Dietz, M. E., & Clausen, J. C. (2005). A Field Evaluation of Rain Garden Flow and Pollutant Treatment. *Water, Air and Soil Pollution*, *167*(1–4), 123–138.

Dietz, M. E., & Clausen, J. C. (2006). Saturation to Improve Pollutant Retention in a Rain Garden. *Environmental Science Technology*, (40), 1335–1340.

Dodds, W. K., Bouska, W. W., Eitzmann, J. L., Pilger, T. J., Pitts, K. L., Riley, A. J., … Thornbrugh, D. J. (2009). Eutrophication of U . S . Freshwaters : Damages. *Environmnetal Science & Technology*, *43*(1), 12–19. https://doi.org/10.1021/es801217q

Dodds, W. K., & Smith, V. H. (2016). Nitrogen , phosphorus , and eutrophication in streams. *Inland Waters*, *6*(2), 155–164. https://doi.org/10.5268/IW-6.2.909

Drapper, D., & Hornbuckle, A. (2018). Removal of Nutrients , Sediment , and Heavy Metals by a Stormwater Treatment Train ; a Medium-Density Residential Case Study in Southeast Queensland. https://doi.org/10.3390/w10101307

Duan, S., Newcomer-Johnson, T., Mayer, P., & Kaushal, S. (2016). Phosphorus Retention in Stormwater Control Structures across Streamflow in Urban and Suburban Watersheds. *Water*, *8*(390), 1–17. https://doi.org/10.3390/w8090390

Duncan, J. M., Band, L. E., Groffman, P. M., & Bernhardt, E. S. (2015). Mechanisms driving the seasonality of catchment scale nitrate export: Evidence for riparian ecohydrologic controls. *Water Resurces Research*, *51*, 3982–3997. https://doi.org/10.1002/2015WR016937.Received

Erickson, A. J., Gulliver, J. S., & Weiss, P. T. (2007). Enhanced Sand Filtration for

Storm Water Phosphorus Removal. *Journal of Environmental Engineering @ASCE*, *133*(5), 485–497.

Erickson, A. J., Gulliver, J. S., & Weiss, P. T. (2012). Capturing phosphates with iron enhanced sand filtration. *Water Research*, *46*(9), 3032–3042. https://doi.org/10.1016/j.watres.2012.03.009

Erickson, A. J., Taguchi, V. J., & Gulliver, J. S. (2018). The Challenge of Maintaining Stormwater Control Measures : A Synthesis of Recent Research and Practitioner Experience. *Sustainability*, *10*(3666), 1–15. https://doi.org/10.3390/su10103666

Frost, P. C., Prater, C., Scott, A. B., Song, K., & Xenopoulos, M. A. (2019). Mobility and Bioavailability of Sediment Phosphorus in Urban Stormwater Ponds Water Resources Research. *Water Resources Research*, *55*, 3680–3688. https://doi.org/10.1029/2018WR023419

Giesler, R., Morth, C.-M., Mellqvist, E., & Torssander, P. (2005). The humus layer determines SO 42 À isotope values in the mineral soil. *Biogeochemistry*, *74*, 3–20. https://doi.org/10.1007/s10533-004-0080-7

Gill, L. W., Ring, P., Higgins, N. M. P., & Johnston, P. M. (2014). Accumulation of heavy metals in a constructed wetland treating road runoff. *Ecological Engineering*, *70*, 133–139. https://doi.org/10.1016/j.ecoleng.2014.03.056

Griffiths, L. N., & Mitsch, W. J. (2017). Removal of nutrients from urban stormwater runoff by storm-pulsed and seasonally pulsed created wetlands in the subtropics. *Ecological Engineering*, *108*, 414–424. https://doi.org/10.1016/j.ecoleng.2017.06.053

Groffman, P. M., Cadenasso, M. L., Cavender-Bares, J., Childers, D. L., Grimm, N. B., Grove, J. M., … Ruddell, B. L. (2017). Moving Towards a New Urban Systems Science. *Ecosystems*, *20*(1), 38–43. https://doi.org/10.1007/s10021-016-0053-4

Hall, S. J., McDowell, W. H., & Silver, W. L. (2013). When Wet Gets Wetter : Decoupling of Moisture , Redox Biogeochemistry , and Greenhouse Gas Fluxes in a Humid Tropical Forest Soil. *Ecosystems*, 576–589. https://doi.org/10.1007/s10021-012-9631-2

Harrison, D. J., & Maynard, D. G. (2014). Nitrogen mineralization assessment using PRS TM probes (ion-exchange membranes) and soil extractions in fertilized and unfertilized pine and spruce soils. *Canadian Journal of Soil Science*, *94*, 21–34. https://doi.org/10.4141/CJSS2012-064

Heisler, J., Glibert, P. M., Burkholder, J. M., Anderson, D. M., Cochlan, W., Dennison, W. C., … Suddleson, M. (2008). Eutrophication and harmful algal blooms : A scientific consensus. *Harmful Algae*, *8*, 3–13. https://doi.org/10.1016/j.hal.2008.08.006

Ho, J. C., & Michalak, A. M. (2017). Phytoplankton blooms in Lake Erie impacted by both long-term and springtime phosphorus loading. *Journal of Great Lakes Research*, *43*(3), 221–228. https://doi.org/10.1016/j.jglr.2017.04.001

Hobbie, S. E., Finlay, J. C., Janke, B. D., Nidzgorski, D. A., Millet, D. B., & Baker, L. A. (2017). Contrasting nitrogen and phosphorus budgets in urban watersheds and implications for managing urban water pollution. *PNAS*, *114*(16), 4177–4182. https://doi.org/10.1073/pnas.1618536114

Howarth, R. W., Sharpley, A., & Walker, D. (2002). Sources of Nutrient Pollution to Coastal Waters in the UnitedStates: Implications for Achieving Coastal Water Quality Goals. *Estuariesuaries*, *25*, 656–676.

Hsieh, C., Davis, A. P., & Needelman, B. A. (2007). Nitrogen Removal from Urban Stormwater Runoff Through Layered Bioretention Columns. *Water Environment Research*, *79*(12), 2404–2411. https://doi.org/10.2175/106143007X183844

Hunt, W. F., ASCE, M., Davis, A. P., ASCE, F., Traver, R. G., & ASCE, M. (2012). Meeting Hydrologic and Water Quality Goals through Targeted Bioretention Design. *Journal of Environmental Engineering*, *138*(6), 698–707. https://doi.org/10.1061/(ASCE)EE.1943-7870.0000504

Hurley, S., Shrestha, P., & Cording, A. (2017). Nutrient Leaching from Compost : Implications for Bioretention and Other Green Stormwater Infrastructure. *Journal of Sustainable Water Built Environmnet*, *3*, 1–8. https://doi.org/10.1061/JSWBAY.0000821

Janke, B. D., Finlay, J. C., & Hobbie, S. E. (2017). Trees and Streets as Drivers of Urban Stormwater Nutrient Pollution. https://doi.org/10.1021/acs.est.7b02225

Jarecke, K. M., Loecke, T. D., & Burgin, A. J. (2016). Soil Biology & Biochemistry Coupled soil oxygen and greenhouse gas dynamics under variable hydrology. *Soil Biology and Biochemistry*, *95*, 164–172. https://doi.org/10.1016/j.soilbio.2015.12.018

Kaye, J. P., Groffman, P. M., Grimm, N. B., Baker, L. A., & Pouyat, R. V. (2006). A distinct urban biogeochemistry ? *TRENDS in Ecology and Evolution*, *21*(4), 192–199. https://doi.org/10.1016/j.tree.2005.12.006

Khan, F. A., & Ansari, A. A. (2005). Eutrophication : An Ecological Vision. *The Botanical Review*, *71*(4), 449–482.

Kim, H., Seagren, E. A., & Davis, A. P. (2003). Engineered Bioretention for Removal of Nitrate from Stormwater Runoff. *Water Environment Research*, *75*(July/August), 355–367.

Krause, H. H., & Ramlal, D. (1987). In Situ Nutrient Extraction by Resin rom Forested, Clear-Cut and Site-Prepared Soil. *Canadian Journal of Soil Science*, *67*(November),

943–952.

Lajtha, K. (1988). The use of ion-exchange resin bags for measuring nutrient availability in an arid ecosystem. *Plant and Soil*, *105*(1), 105–111. https://doi.org/10.1007/BF02371147

Langenhove, L. Van, Janssens, I. A., Verryckt, L., Brechet, L., Hartley, I. P., Stahl, C., … Grau, O. (2020). Rapid root assimilation of added phosphorus in a lowland tropical rainforest of French Guiana. *Soil Biology & Biogeochemistry*, *140*(November 2019), 2019–2021. https://doi.org/10.1016/j.soilbio.2019.107646

LeFevre, G. H., Asce, S. M., Paus, K. H., Natarajan, P., Gulliver, J. S., ASCE, F., … Hozalski, R. M. (2015). Review of Dissolved Pollutants in Urban Storm Water and Their Removal and Fate in Bioretention Cells. *Journal of Environmental Engineering*, *141*(1). https://doi.org/10.1061/(ASCE)EE.1943-7870.0000876.

Li, J., & Davis, A. P. (2016). A unified look at phosphorus treatment using bioretention. *Water Research*, *90*, 141–155. https://doi.org/10.1016/j.watres.2015.12.015

Li, L., & Davis, A. P. (2014). Urban Stormwater Runo ff Nitrogen Composition and Fate in Bioretention Systems. *Environmental Science & Technology*, *48*, 3403–3410. https://doi.org/10.1021/es4055302

Lintern, A., McPhillips, L., Winfrey, B., Duncan, J., & Grady, C. (2020). Best Management Practices for Di ff use Nutrient Pollution : Wicked Problems Across Urban and Agricultural Watersheds. *Environmnetal Science & Technology*. https://doi.org/10.1021/acs.est.9b07511

Lucas, W. C., & Greenway, M. (2008). Nutrient Retention in Vegetated and Nonvegetated Bioretention Mesocosms. *Journal of Irrigation and Drainage Enginering*, *134*(5), 613–623. https://doi.org/10.1061/(ASCE)0733-9437(2008)134

Lucas, W. C., & Greenway, M. (2011). Hydraulic Response and Nitrogen Retention in Bioretention Mesocosms with Regulated Outlets : Part II — Nitrogen Retention. *Water Environment Research*, *83*(8), 703–713. https://doi.org/10.2175/106143011X12989211840936

Lucas, W. C., & Sample, D. J. (2015). Reducing combined sewer overflows by using outlet controls for Green Stormwater Infrastructure : Case study in Richmond , Virginia. *Journal of Hydrology*, *520*, 473–488. https://doi.org/10.1016/j.jhydrol.2014.10.029

Lundell, Y. (1989). In situ ion exchange resin bags to estimate forest site quality. *Plant and Soil*, *119*, 186–190.

Lundell, Ylva. (2001). Soil Nutrient A vailability A ssessed by In Situ Ion-exchange Resin Bags as a Predictor of Growth of Swedish Coniferous. *Scandanavian Journal of Forest Research*, *16*, 260–268.

Martinsen, V., Mulder, J., Shitumbanuma, V., Sparrevik, M., Borresen, T., & Cornelissen, G. (2014). Farmer-led maize biochar trials: Effect on crop yield and soil nutrients under conservation farming. *Journal of Plant Nutrition and Soil Science*, *177*(5), 681–695. https://doi.org/10.1002/jpln.201300590

McGrath, D. A., Comerford, N. B., & Duryea, M. L. (2000). Litter dynamics and monthly fluctuations in soil phosphorus availability in an Amazonian agroforest. *Forest Ecology and Management*, *131*, 167–181.

Mcphillips, L. E., Groffman, P. M., Schneider, R. L., & Walter, M. T. (2016). Nutrient Cycling in Grassed Roadside Ditches and Lawns in a Suburban Watershed. *Journal of Environmnetal Quality*. https://doi.org/10.2134/jeq2016.05.0178

McPhillips, L., Ph, D., Goodale, C., Ph, D., Walter, M. T., Ph, D., & Asce, M. (2018). Nutrient Leaching and Greenhouse Gas Emissions in Grassed Detention and Bioretention Stormwater Basins. *Journal of Sustainable Water Built Environment*, *4*(1), 1–10. https://doi.org/10.1061/JSWBAY.0000837.

McPhillips, L., & Walter, M. T. (2015). Hydrologic conditions drive denitrification and greenhouse gas emissions in stormwater detention basins. *Ecological Engineering*, *85*, 67–75. https://doi.org/10.1016/j.ecoleng.2015.10.018

Meason, D. F., & Idol, T. W. (2008). Nutrient Sorption Dynamics of Resin Membranes and Resin Bags in a Tropical Forest. *Soil Science Society America Journal*, *72*(6), 1806–1814. https://doi.org/10.2136/sssaj2008.0010

Michalak, A. M., Anderson, E. J., Beletsky, D., Boland, S., Bosch, N. S., Bridgeman, T. B., … Scavia, D. (2013). Record-setting algal bloom in Lake Erie caused by agricultural and meteorological trends consistent with expected future conditions, *110*(16). https://doi.org/10.1073/pnas.1216006110

Miller, E. M., & Seastedt, T. R. (2009). Forest Ecology and Management Impacts of woodchip amendments and soil nutrient availability on understory vegetation establishment following thinning of a ponderosa pine forest. *Forest Ecology and Management*, *258*, 263–272. https://doi.org/10.1016/j.foreco.2009.04.011

Miller, J. J., Bremer, E., & Curtis, T. (2016). Influence of Organic Amendment and Compaction on Nutrient Dynamics in a Saturated Saline-Sodic Soil from the Riparian Zone. *Journal of Environmental Quality*, *45*(4), 1437–1444. https://doi.org/10.2134/jeq2016.01.0033

Morse, N. R., McPhillips, L. E., Shapleigh, J. P., & Walter, M. T. (2017). The Role of Denitrification in Stormwater Detention Basin Treatment of Nitrogen. *Environmental Science & Technology*, *51*, 7928–7935. https://doi.org/10.1021/acs.est.7b01813

Mulholland, J. (1997). Seasonal patterns in streamwater nutrient and dissolved organic carbon concentrations : Separating catchment flow path, *33*(6), 1297–1306.

Mullins, A. R., Bain, D. J., Pfeil-mccullough, E., Hopkins, K. G., Lavin, S., & Copeland, E. (2020). Seasonal drivers of chemical and hydrological patterns in roadside in fi ltration-based green infrastructure. *Science of the Total Environment*, *714*, 136503. https://doi.org/10.1016/j.scitotenv.2020.136503

Murdoch, P. S., & Stoddard, J. L. (1992). The Role of Nitrate in the Acidification of Streams in the Catskill Mountains of New York. *Water Resurces Research*, *28*(10), 2707–2720.

NAE Grand Challenges. (n.d.). Retrieved from http://www.engineeringchallenges.org/challenges.aspx

Nidizgorski, D. A., & Hobbie, S. E. (2016). Urban trees reduce nutrient leaching to groundwater. *Ecological Applications*, *26*(5), 1566–1580.

Norby, R. J., Sloan, V. L., Iversen, C. M., & Childs, J. (2019). Controls on Fine-Scale Spatial and Temporal Variability of Plant- Available Inorganic Nitrogen in a Polygonal Tundra Landscape. *Ecosystems*, *22*(3), 528–543. https://doi.org/10.1007/s10021-018-0285-6

Norton, R. A., Harrison, J. A., Keller, C. K., & Moffett, K. B. (2017). Effects of storm size and frequency on nitrogen retention , denitrification , and N 2 O production in bioretention swale mesocosms. *Biogeochemistry*, (134), 353–370. https://doi.org/10.1007/s10533-017-0365-2

Olila, O. G., Reddy, K. R., & Stites, D. L. (1997). Influence of draining on soil phosphorus forms and distribution in a constructed wetland, *9*, 157–169.

Pampolino, M. F., & Hatano, R. (2000). Soil Science and Plant Nutrition Comparison between conventional soil tests and the use of resin capsules for measuring P , K , and N in two soils under two moisture conditions. *Soil Science and Plant Nutrition*, *64*(2), 461–471.

Pataki, D. E., Carreiro, M. M., Cherrier, J., Grulke, N. E., Jennings, V., Pincetl, S., … Zipperer, W. C. (2011). Coupling biogeochemical cycles in urban environments : ecosystem services , green solutions , and misconceptions. *Frontiers in Ecology*, *9*(1), 27–36. https://doi.org/10.1890/090220

Patterson, J. J., Smith, C., & Bellamy, J. (2013). Understanding enabling capacities for managing the ‘ wicked problem ’ of nonpoint source water pollution in catchments : A conceptual framework. *Journal of Environmental Management*, *128*, 441–452. https://doi.org/10.1016/j.jenvman.2013.05.033

Porporato, A., & Odorico, P. D. Õ. (2003). Hydrologic controls on soil carbon and nitrogen cycles . I . Modeling scheme. *Advances in Water Resources*, *26*, 45–58.

Pouyat, R. V, Forest, U., Yesilonis, I. D., & Forest, U. (2007). Nitrate Leaching and Nitrous Oxide Flux in Urban Forests and Grasslands. *Rechnical Reports: Landscape*

and Watershed Processes, 1848–1860. https://doi.org/10.2134/jeq2008.0521

PRS Technology. (2020). Retrieved from https://www.westernag.ca/innovations/technology

Qian, P., & Schoenau, J. J. (2002). Practical applications of ion exchange resins in agricultural and environmental soil research. *Canadian Journal of Soil Science*, *82*(1), 9–21. https://doi.org/10.4141/S00-091

Qian, P., & Schoenau, J. J. (2007). Using an Anion Exchange Membrane to Predict Soil Available N and S Supplies and the Impact of N and S Fertilization on Canola and Wheat Growth, *17*(1), 77–83.

Roseen, Robert, M., Ballestero, Thomas, P., Houle, James, J., Avellaneda, P., Briggs, J., Fowler, G., & Wildey, R. (2009). Seasonal Performance Variations for Storm-Water Management Systems in Cold Climate Conditions. *Journal of Environmental Engineering*, *135*(March), 128–137. https://doi.org/10.1061/(ASCE)0733-9372(2009)135

Schindler, D. W., Carpenter, S. R., Chapra, S. C., Hecky, R. E., & Orihel, D. M. (2016). Reducing Phosphorus to Curb Lake Eutrophication is a Success. *Environmnetal Science & Technology*, *50*, 8923–8929. https://doi.org/10.1021/acs.est.6b02204

Selbig, W. R. (2016). Science of the Total Environment Evaluation of leaf removal as a means to reduce nutrient concentrations and loads in urban stormwater. *Science of the Total Environment, The*, *571*, 124–133. https://doi.org/10.1016/j.scitotenv.2016.07.003

Sevostianova, E., & Leinauer, B. (2014). Subsurface-Applied Tailored Water : Combining Nutrient Benefits with Efficient Turfgrass Irrigation. *Crop Science*, *54*(october), 1926–1938. https://doi.org/10.2135/cropsci2014.01.0014

Sharifi, M., Lynch, D. H., Zebarth, B. J., Zheng, Z., & Martin, R. C. (2009). Evaluation of Nitrogen Supply Rate Measured by in situ Placement of Plant Root Simulator ™ Probes as a Predictor of Nitrogen Supply from Soil and Organic Amendments in Potato Crop. *American Journal of Potato Research*, *86*, 356–366. https://doi.org/10.1007/s12230-009-9090-2

Sharior, S., McDonald, W., & Parolari, A. J. (2019). Improved reliability of stormwater detention basin performance through water quality data-informed real-time control. *Journal of Hydrology*, *573*(March), 422–431. https://doi.org/10.1016/j.jhydrol.2019.03.012

Smyth, A. R., Loecke, T. D., Franz, T. E., & Burgin, A. J. (2019). Using high-frequency soil oxygen sensors to predict greenhouse gas emissions from wetlands. *Soil Biology and Biochemistry*, *128*(July 2018), 182–192. https://doi.org/10.1016/j.soilbio.2018.10.020

Sohn, W., Kim, J., Li, M., & Brown, R. (2019). The influence of climate on the effectiveness of low impact development : A systematic review. *Journal of Environmental Management*, *236*(February), 365–379. https://doi.org/10.1016/j.jenvman.2018.11.041

Song, K., Winters, C., Xenopoulos, M. A., Marsalek, J., & Frost, P. C. (2017). Phosphorus cycling in urban aquatic ecosystems: connecting biological processes and water chemistry to sediment P fractions in urban stormwater management ponds. *Biogeochemistry*, *132*, 203–212. https://doi.org/https://doi.org/10.1007/s10533-017-0293-1

Song, K., Xenopoulos, M. A., Marsalek, J., & Frost, P. C. (2015). The fingerprints of urban nutrients: dynamics of phosphorus speciation in water flowing through developed landscapes. *Biogeochemistry*, *125*, 1–10. Retrieved from https://doi.org/10.1007/s10533-015-0114-3

Stets, E. G., Sprague, L. A., Oelsner, G. P., Johnson, H. M., Murphy, J. C., Ryberg, K., … Riskin, M. L. (2020). Landscape Drivers of Dynamic Change in Water Quality of U.S. Rivers. *Environmental Sceince and Technology*, *54*, 4436–4343. https://doi.org/10.1021/acs.est.9b05344

Sustainable Development Goals. (2020). Retrieved from https://www.undp.org/content/undp/en/home/sustainable-development-goals.html#:~:text=The Sustainable Development Goals (SDGs,peace and prosperity by 2030.

Switzer, J. M., Hope, G. D., Grayston, S. J., & Prescott, C. E. (2012). Forest Ecology and Management Changes in soil chemical and biological properties after thinning and prescribed fire for ecosystem restoration in a Rocky Mountain Douglas-fir forest. *Forest Ecology and Management*, *275*, 1–13. https://doi.org/10.1016/j.foreco.2012.02.025

Trentman, M. T., Tank, J. L., Jones, S. E., Mcmillan, S. K., & Royer, T. V. (2020). Science of the Total Environment Seasonal evaluation of biotic and abiotic factors suggests phosphorus retention in constructed fl oodplains in three agricultural streams. *Science of the Total Environment*, *729*, 138744. https://doi.org/10.1016/j.scitotenv.2020.138744

Tzoulas, K., Korpela, K., Venn, S., Yli-pelkonen, V., Ka, A., Niemela, J., & James, P. (2007). Promoting ecosystem and human health in urban areas using Green Infrastructure : A literature review. *Landscape and Urban Planning*, *81*, 167–178. https://doi.org/10.1016/j.landurbplan.2007.02.001

Van Meter, K. J., Chowdhury, S., Byrnes, D. K., & Basu, N. B. (2019). Biogeochemical asynchrony : Ecosystem drivers of seasonal concentration regimes across the Great Lakes Basin. *Limnology and Oceaonography*, 1–15. https://doi.org/10.1002/lno.11353

Walaszek, M., Bois, P., Laurent, J., Lenormand, E., & Wanko, A. (2018). Urban stormwater treatment by a constructed wetland : Seasonality impacts on hydraulic ef fi ciency , physico-chemical behavior and heavy metal occurrence. *Science of the Total Environment*, *637–638*, 443–454. https://doi.org/10.1016/j.scitotenv.2018.04.325

Walker, D. J., & Hurl, S. (2002). The reduction of heavy metals in a stormwater wetland. *Ecological Engineering*, *18*, 407–414.

Wang, W., Haver, D., & Pataki, D. E. (2014). Nitrogen budgets of urban lawns under three different management regimes in southern California, 127–148. https://doi.org/10.1007/s10533-013-9942-1

Weatherburn, M. W. (1967). Phenol-Hypochlorite Reaction for Determination of Ammonia. *Analytical Chemistry*, *39*(8), 971–974. https://doi.org/10.1021/ac60252a045

Wines, M. (2014, August 4). Behind Toledo's Water Crisis, a Long-Troubled Lake Erie. *The New York Times*. Retrieved from https://www.nytimes.com/2014/08/05/us/lifting-ban-toledo-says-its-water-is-safe-to-drink-again.html

Yan, Q., Davis, A. P., Asce, F., & James, B. R. (2016). Enhanced Organic Phosphorus Sorption from Urban Stormwater Using Modified Bioretention Media : Batch Studies, *142*(4), 1–11. https://doi.org/10.1061/(ASCE)EE.1943-7870.0001073

You, Z., Zhang, L., Pan, S., Chiang, P., Pei, S., & Zhang, S. (2019). Performance evaluation of modified bioretention systems with alkaline solid wastes for enhanced nutrient removal from stormwater runoff. *Water Research*, *161*, 61–73. https://doi.org/10.1016/j.watres.2019.05.105

8. APPENDIX

Table A1: Seasonality of Environmental Drivers at the West Garden. Air temperature, soil temperature, soil moisture and soil oxygen are two-week averages, where air temperature is based off daily data and the other three factors are averaged from continuous 5-minute data. Precipitation is a cumulative two-week sum of daily precipitation.

Interval	Start	End	T_A (°F)	T_S (°F)	VWC (%)	O2 (%)	P (in)
1	4/15/2019	4/29/2019	49.32	52.76	0.28	0.18	1.49
2	4/29/2019	5/13/2019	47.79	51.50	0.33	0.19	2.72
3	5/13/2019	5/27/2019	57.04	59.00	0.30	0.18	4.04
4	5/27/2019	6/10/2019	59.87	62.80	0.26	0.18	1.24
5	6/10/2019	6/24/2019	61.42	66.59	0.22	0.19	2.20
6	6/24/2019	7/8/2019	73.68	76.00	0.22	0.18	1.70
7	7/8/2019	7/22/2019	76.13	77.83	0.11	0.19	2.84
8	7/22/2019	8/5/2019	73.20	76.08	0.10	0.19	0.25
9	8/5/2019	8/19/2019	73.46	74.53	0.09	0.18	1.58
10	8/19/2019	9/2/2019	69.70	71.15	0.09	0.19	1.70
11	9/2/2019	9/16/2019	67.43	67.80	0.13	0.19	5.06
12	9/16/2019	9/30/2019	67.30	68.00	0.20	0.19	1.94

Table A2: Seasonality of Environmental Drivers at the East Garden. Air temperature, soil temperature, soil moisture and soil oxygen are two-week averages, where air temperature is based off daily data and the other three factors are averaged from continuous 5-minute data. Precipitation is a cumulative two-week sum of daily precipitation.

Interval	Start	End	T_A (°F)	T_S (°F)	VWC (%)	O2 (%)	P (in)
1	4/15/2019	4/29/2019	49.32	53.43	0.38	0.17	1.49
2	4/29/2019	5/13/2019	47.79	51.64	0.43	0.17	2.72
3	5/13/2019	5/27/2019	57.04	59.97	0.42	0.17	4.04
4	5/27/2019	6/10/2019	59.87	65.76	0.43	0.16	1.24
5	6/10/2019	6/24/2019	61.42	64.99	0.38	0.17	2.20
6	6/24/2019	7/8/2019	73.68	73.44	0.37	0.16	1.70
7	7/8/2019	7/22/2019	76.13	75.17	0.29	0.17	2.84
8	7/22/2019	8/5/2019	73.20	72.60	0.28	0.17	0.25
9	8/5/2019	8/19/2019	73.46	71.94	0.24	0.17	1.58
10	8/19/2019	9/2/2019	69.70	70.93	0.22	0.17	1.70
11	9/2/2019	9/16/2019	67.43	67.98	0.25	0.17	5.06
12	9/16/2019	9/30/2019	67.30	68.67	0.26	0.17	1.94

Table A3: Seasonality of Environmental Drivers at the Green Roof. Air temperature, soil temperature, soil moisture and soil oxygen are two-week averages, where air temperature is based off daily data and the other three factors are averaged from continuous 5-minute data. Precipitation is a cumulative two-week sum of daily precipitation. Missing Data points are due to a delay between the installation of auto sampling tools and the beginning of nutrient observation.

Interval	Start	End	T_A (°F)	T_S (°F)	VWC (%)	O2 (%)	P (in)
1	4/18/2019	5/2/2019	48.67	-	-	-	2.58
2	5/2/2019	5/16/2019	51.25	-	-	-	1.70
3	5/16/2019	5/30/2019	56.60	-	-	-	4.25
4	5/30/2019	6/13/2019	61.46	-	-	-	2.20
5	6/13/2019	6/27/2019	63.46	63.85	0.14	0.19	1.48
6	6/27/2019	7/11/2019	73.81	74.17	0.12	0.19	1.12
7	7/11/2019	7/25/2019	75.50	75.75	0.11	0.19	2.84
8	7/25/2019	8/8/2019	74.43	74.04	0.09	0.19	1.20
9	8/8/2019	8/22/2019	73.11	72.72	0.09	0.19	0.64
10	8/22/2019	9/5/2019	68.26	68.01	0.09	0.19	1.95
11	9/5/2019	9/19/2019	67.38	67.80	0.14	0.19	4.80
12	9/19/2019	10/3/2019	67.12	66.51	0.14	0.19	4.65

Table A4: Seasonality of Environmental Drivers at the Wetland Upland. Air temperature, soil temperature, soil moisture and soil oxygen are two-week averages, where air temperature is based off daily data and the other three factors are averaged from continuous 5-minute data. Precipitation is a cumulative two-week sum of daily precipitation. Missing Data points are due to a delay between the installation of auto sampling tools and the beginning of nutrient observation.

Interval	Start	End	T_A (°F)	T_S (°F)	VWC (%)	O2 (%)	P (in)
1	4/24/2019	5/8/2019	46.75	-	-	-	2.51
2	5/8/2019	5/22/2019	51.46	-	-	-	2.72
3	5/22/2019	6/5/2019	60.42	62.92	0.40	0.14	3.19
4	6/5/2019	6/19/2019	61.29	66.44	0.37	0.18	1.91
5	6/19/2019	7/3/2019	69.56	70.05	0.38	0.18	2.24
6	7/3/2019	7/17/2019	74.63	74.89	0.25	0.19	0.03
7	7/17/2019	7/31/2019	75.65	74.92	0.27	0.19	2.84
8	7/31/2019	8/14/2019	73.08	73.16	0.22	0.19	1.39
9	8/14/2019	8/28/2019	71.19	71.30	0.18	0.20	2.14
10	8/28/2019	9/11/2019	67.12	67.50	0.21	0.20	1.70
11	9/11/2019	9/25/2019	69.18	69.03	0.34	0.19	3.90
12	9/25/2019	10/9/2019	60.90	63.51	0.37	0.19	4.31

Table A5: Seasonality of Environmental Drivers at the Wetland Lowland. Air temperature, soil temperature, soil moisture and soil oxygen are two-week averages, where air temperature is based off daily data and the other three factors are averaged from continuous 5-minute data. Precipitation is a cumulative two-week sum of daily precipitation. Missing Data points are due to a delay between the installation of auto sampling tools and the beginning of nutrient observations.

Interval	Start	End	T_A (°F)	T_S (°F)	VWC (%)	O2 (%)	P (in)
1	4/24/2019	5/8/2019	46.75	-	-	-	2.51
2	5/8/2019	5/22/2019	51.46	-	-	-	2.72
3	5/22/2019	6/5/2019	60.42	63.49	0.44	0.17	3.19
4	6/5/2019	6/19/2019	61.29	66.12	0.43	0.14	1.91
5	6/19/2019	7/3/2019	69.56	70.22	0.44	0.13	2.24
6	7/3/2019	7/17/2019	74.63	75.68	0.43	0.05	0.03
7	7/17/2019	7/31/2019	75.65	75.40	0.42	0.09	2.84
8	7/31/2019	8/14/2019	73.08	72.39	0.42	0.15	1.39
9	8/14/2019	8/28/2019	71.19	70.69	0.40	0.14	2.14
10	8/28/2019	9/11/2019	67.12	67.17	0.42	0.13	1.70
11	9/11/2019	9/25/2019	69.18	68.85	0.43	0.02	3.90
12	9/25/2019	10/9/2019	60.90	63.66	0.43	0.01	4.31

Table A6: Nutrient Availability in the West Garden. Nitrate, ammonium, and phosphate observed as cumulative measurements of available nutrients over a two-week monitoring period. Nutrient availability measured by IER Bags are in units of mass analyte per mass resin per burial period, whereas measurements with IEMs are in mass analyte per surface area of resin per burial period. Asterisks note readings below the detection limit.

Interval	1	2	3	4	5	6	7	8	9	10	11	12
Start Date	4/15/2019	4/29/2019	5/13/2019	5/27/2019	6/10/2019	6/24/2019	7/8/2019	7/22/2019	8/5/2019	8/19/2019	9/2/2019	9/16/2019
End Date	4/29/2019	5/13/2019	5/27/2019	6/10/2019	6/24/2019	7/8/2019	7/22/2019	8/5/2019	8/19/2019	9/2/2019	9/16/2019	9/30/2019
IER Bag (µg· 5-gram resin^{-1} ·2-weeks^{-1})												
NO3	1261.56	860.63	1890.42	894.39	2796.83	1430.56	1841.65	340.01	1249.30	1619.42	1261.18	598.56
NH4	100.88	26.71	92.71	98.65	42.44	64.68	144.45	67.27	33.59	108.99	66.10	72.01
PO4	109.83	121.84	233.45	222.07	276.33	125.09	439.12	99.04	226.29	309.53	316.51	157.52
IEM (µg· 17.5cm^2 resin^{-1} ·2-weeks^{-1})												
NO3-N	414.28	216.06	369.44	395.72	612.24	553.54	241.02	85.86	164.42	164.64	183.76	132.74
NH4-N	1.72*	3.72	1.22*	0.00*	6.16	1.88*	4.32	1.84*	9.34	7.06	5.74	11.06
PO4	18.49	31.16	51.60	24.83	57.40	24.61	39.32	25.07	43.18	33.57	43.75	36.68

Table A7: Nutrient Availability in the East Garden. Nitrate, ammonium, and phosphate observed as cumulative measurements of available nutrients over a two-week monitoring period. Nutrient availability measured by IER Bags are in units of mass analyte per mass resin per burial period, whereas measurements with IEMs are in mass analyte per surface area of resin per burial period. Asterisks note readings below the detection limit.

Interval	**1**	**2**	**3**	**4**	**5**	**6**	**7**	**8**	**9**	**10**	**11**	**12**
Start Date	4/15/2019	4/29/2019	5/13/2019	5/27/2019	6/10/2019	6/24/2019	7/8/2019	7/22/2019	8/5/2019	8/19/2019	9/2/2019	9/16/2019
End Date	4/29/2019	5/13/2019	5/27/2019	6/10/2019	6/24/2019	7/8/2019	7/22/2019	8/5/2019	8/19/2019	9/2/2019	9/16/2019	9/30/2019
IER Bag (µg· 5-gram resin^{-1} ·2-weeks^{-1})												
NO3	1870.06	879.17	2327.27	943.40	1989.11	1893.96	1001.25	374.22	587.24	484.46	701.46	721.90
NH4	111.66	62.09	40.69	75.73	48.53	77.70	83.84	95.75	83.31	69.30	59.60	53.12
PO4	148.02	165.53	231.64	235.99	291.21	233.43	288.43	99.58	229.12	274.03	324.35	145.85
IEM (µg· 17.5cm^2 resin^{-1} ·2-weeks^{-1})												
NO3-N	704.24	313.52	445.28	584.38	507.74	313.34	177.04	47.62	132.96	46.22	132.68	242.14
NH4-N	1.58*	2.24	5.74	0.00*	9.32	2.92	5.16	3.34	6.56	5.46	12.34	9.10
PO4	18.09	32.00	39.61	24.33	37.04	30.53	42.76	17.82	47.87	58.11	57.55	31.48

Table A8: Nutrient Availability in the Green Roof. Nitrate, ammonium, and phosphate observed as cumulative measurements of available nutrients over a two-week monitoring period. Nutrient availability measured by IER Bags are in units of mass analyte per mass resin per burial period, whereas measurements with IEMs are in mass analyte per surface area of resin per burial period. Asterisks note readings below the detection limit.

Interval	**1**	**2**	**3**	**4**	**5**	**6**	**7**	**8**	**9**	**10**	**11**	**12**
Start Date	4/18/2019	5/2/2019	5/16/2019	5/30/2019	6/13/2019	6/27/2019	7/11/2019	7/25/2019	8/8/2019	8/22/2019	9/5/2019	9/19/2019
End Date	5/2/2019	5/16/2019	5/30/2019	6/13/2019	6/27/2019	7/11/2019	7/25/2019	8/8/2019	8/22/2019	9/5/2019	9/19/2019	10/3/2019
IER Bag (µg· 5-gram resin^{-1} ·2-weeks^{-1})												
NO3	59.77	103.65	76.96	504.28	21.89	149.95	616.43	617.92	116.66	376.57	460.79	217.12
NH4	20.25	2.88	13.36	72.21	57.62	58.48	102.35	102.07	93.46	89.96	49.12	122.69
PO4	97.08	31.53	61.54	59.96	60.28	66.22	188.34	103.60	43.17	126.94	139.86	93.22
IEM (µg· 17.5cm^2 resin^{-1} ·2-weeks^{-1})												
NO3-N	13.64	5.32	18.06	7.62	4.48	9.00	18.28	20.98	13.16	12.52	16.30	28.26
NH4-N	3.26	10.84	5.42	0.00*	7.00	7.46	3.64	2.68	3.18	4.64	7.98	2.34
PO4	3.91	4.16	10.72	4.28	8.66	5.58	10.18	2.78	5.79	5.86	10.37	18.78

Table A9: Nutrient Availability in the Wetland Upland. Nitrate, ammonium, and phosphate observed as cumulative measurements of available nutrients over a two-week monitoring period. Nutrient availability measured by IER Bags are in units of mass analyte per mass resin per burial period, whereas measurements with IEMs are in mass analyte per surface area of resin per burial period. Asterisks note readings below the detection limit. Italics note an average value between two replicates rather than three due to an outlier.

Interval	**1**	**2**	**3**	**4**	**5**	**6**	**7**	**8**	**9**	**10**	**11**	**12**
Start Date	4/24/2019	5/8/2019	5/22/2019	6/5/2019	6/19/2019	7/3/2019	7/17/2019	7/31/2019	8/14/2019	8/28/2019	9/11/2019	9/25/2019
End Date	5/8/2019	5/22/2019	6/5/2019	6/19/2019	7/3/2019	7/17/2019	7/31/2019	8/14/2019	8/28/2019	9/11/2019	9/25/2019	10/9/2019
IER Bag (µg· 5-gram resin^{-1} ·2-weeks^{-1})												
NO3	18.15	390.86	79.82	113.37	46.90	73.86	144.27	260.22	57.23	142.43	98.96	127.61
NH4	72.43	41.12	21.60	68.31	128.08	121.15	125.58	73.42	103.87	105.27	171.53	*72.02*
PO4	59.51	68.04	50.04	62.12	70.09	32.15	174.00	71.26	92.91	40.81	116.40	143.70
IEM (µg· 17.5cm^2 resin^{-1} ·2-weeks^{-1})												
NO3-N	24.20	22.10	3.90	3.24	1.64*	3.20	4.28	7.44	4.66	8.72	3.64	5.30
NH4-N	2.02	3.76	0.00*	5.40	6.02	4.96	10.36	0.46*	1.08*	3.56	2.12	0.70*
PO4	6.90	9.30	7.23	9.06	9.07	3.8	16.2	6.0	13.80	6.28	9.43	11.23

Table A10: Nutrient Availability in the Wetland Lowland. Nitrate, ammonium, and phosphate observed as cumulative measurements of available nutrients over a two-week monitoring period. Nutrient availability measured by IER Bags are in units of mass analyte per mass resin per burial period, whereas measurements with IEMs are in mass analyte per surface area of resin per burial period. Asterisks note readings below the detection limit.

Interval	1	2	3	4	5	6	7	8	9	10	11	12
Start Date	4/24/2019	5/8/2019	5/22/2019	6/5/2019	6/19/2019	7/3/2019	7/17/2019	7/31/2019	8/14/2019	8/28/2019	9/11/2019	9/25/2019
End Date	5/8/2019	5/22/2019	6/5/2019	6/19/2019	7/3/2019	7/17/2019	7/31/2019	8/14/2019	8/28/2019	9/11/2019	9/25/2019	10/9/2019
IER Bag (µg· 5-gram resin^{-1} ·2-weeks^{-1})												
NO3	32.98	350.26	85.25	297.98	429.61	583.32	154.81	420.36	290.72	91.16	98.32	112.56
NH4	153.74	42.14	81.17	92.12	77.46	72.54	133.84	85.80	48.50	187.38	53.10	51.38
PO4	12.30	27.82	21.76	55.17	44.90	16.31	57.46	52.35	37.95	29.98	37.30	19.80
IEM (µg· 17.5cm^2 resin^{-1} ·2-weeks^{-1})												
NO3-N	7.54	4.52	5.90	10.38	2.20	39.40	18.90	55.16	5.72	8.40	4.46	6.88
NH4-N	0.36*	4.62	4.54	0.00*	4.96	5.72	2.74	5.28	3.70	4.24	1.08*	0.76*
PO4	0.31	1.22	2.84	1.58	4.25	4.76	5.02	3.06	2.60	5.25	1.67	2.38

Table A 11: Nutrients extracted from blank IER Bags not deployed in the field. A single blank was used for the first four observation intervals. From the fifth interval to the end of the study, three blanks were analyzed per interval, starting and ending on the same day that an IER bag was deployed and retrieved from each of the field sites.

Interval	**1**	**2**	**3**	**4**	**5**	**6**	**7**	**8**	**9**	**10**	**11**	**12**
Nitrate (µg· 5-gram resin^{-1} ·2-weeks^{-1})												
Garden	-	-	-	-	0.00	35.32	138.50	280.75	105.62	247.15	0.00	0.00
Green Roof	-	-	-	-	401.47	2058.91	91.97	632.31	196.86	0.00	237.71	72.67
Wetland	-	-	-	-	304.80	766.22	929.13	106.95	83.62	136.31	124.84	199.37
Shared	0.00	63.56	0.00	614.23	-	-	-	-	-	-	-	-
Ammonium (µg· 5-gram resin^{-1} ·2-weeks^{-1})												
Garden	-	-	-	-	0.76	46.97	42.40	25.32	25.06	61.04	0.00	45.36
Green Roof	-	-	-	-	7.41	44.69	47.43	35.98	33.71	0.00	35.61	37.99
Wetland	-	-	-	-	4.41	39.35	33.84	43.68	22.80	46.51	100.32	21.99
Shared	0.00	0.00	69.54	50.33	-	-	-	-	-	-	-	-
Phosphate (µg· 5-gram resin^{-1} ·2-weeks^{-1})												
Garden	-	-	-	-	104.46	30.20	226.99	54.01	42.18	9.91	0.00	4.77
Green Roof	-	-	-	-	109.51	72.47	167.32	57.16	80.00	0.00	18.78	6.66
Wetland	-	-	-	-	7.02	17.41	9.68	3.54	3.05	9.91	15.51	2.33
Shared	23.73	19.38	8.06	16.66	-	-	-	-	-	-	-	-

Table A 12: Evaluation of collinearity between independent variables at the West Garden. Collinearity was determined with coefficient of determination, where collinearity between variables is considered high for values above 0.10.

	Time	**Precipitation**	**VWC**	**T_A**	**T_S**	**O_2**
Time	-	0.00	0.63	0.56	0.47	0.06
Precipitation	-	-	0.02	0.03	0.05	0.00
VWC	-	-	-	0.74	0.71	0.12
T_A	-	-	-	-	0.98	0.01
T_S	-	-	-	-	-	0.02
O_2	-	-	-	-	-	-

Table A 13: Evaluation of collinearity between independent variables at the East Garden. Collinearity was determined with coefficient of determination, where collinearity between variables is considered high for values above 0.10.

	Time	**Precipitation**	**VWC**	**T_A**	**T_S**	**O_2**
Time	-	0.00	0.80	0.56	0.53	0.00
Precipitation	-	-	0.00	0.03	0.04	0.04
VWC	-	-	-	0.51	0.44	0.06
T_A	-	-	-	-	0.97	0.13
T_S	-	-	-	-	-	0.19
O_2	-	-	-	-	-	-

Table A 14: Evaluation of collinearity between independent variables at the Green Roof. Collinearity was determined with coefficient of determination, where collinearity between variables is considered high for values above 0.10.

	Time	**Precipitation**	**VWC**	**T_A**	**T_S**	**O_2**
Time	-	0.46	0.01	0.04	0.06	0.64
Precipitation	-	-	0.45	0.15	0.15	0.17
VWC	-	-	-	0.42	0.37	0.07
T_A	-	-	-	-	0.99	0.14
T_S	-	-	-	-	-	0.10
O_2	-	-	-	-	-	-

Table A 15: Evaluation of collinearity between independent variables at the Wetland Upland. Collinearity was determined with coefficient of determination, where collinearity between variables is considered high for values above 0.10.

	Time	**Precipitation**	**VWC**	**T_A**	**T_S**	**O_2**
Time	-	0.15	0.13	0.01	0.00	0.42
Precipitation	-	-	0.30	0.25	0.36	0.08
VWC	-	-	-	0.43	0.40	0.51
T_A	-	-	-	-	0.95	0.32
T_S	-	-	-	-	-	0.33
O_2	-	-	-	-	-	-

Table A 16: Evaluation of collinearity between independent variables at the Wetland Lowland. Collinearity was determined with coefficient of determination, where collinearity between variables is considered high for values above 0.10.

	Time	**Precipitation**	**VWC**	**T_A**	**T_S**	**O_2**
Time	-	0.15	0.15	0.01	0.00	0.38
Precipitation	-	-	0.10	0.25	0.35	0.11
VWC	-	-	-	0.17	0.11	0.04
T_A	-	-	-	-	0.94	0.01
T_S	-	-	-	-	-	0.01
O_2	-	-	-	-	-	-